HHS Public Access

Author manuscript

JACC Cardiovasc Imaging. Author manuscript; available in PMC 2018 July 01.

Published in final edited form as:

JACC Cardiovasc Imaging. 2017 July ; 10(7): 797–818. doi:10.1016/j.jcmg.2017.04.003.

Radiation Safety in Children With Congenital and Acquired Heart Disease:

A Scientific Position Statement on Multimodality Dose Optimization From the Image Gently Alliance

Kevin D. Hill, MD, MS[a], **Donald P. Frush, MD**[b], **B. Kelly Han, MD**[c], **Brian G. Abbott, MD**[d], **Aimee K. Armstrong, MD**[e], **Robert A. DeKemp, PhD**[f], **Andrew C. Glatz, MD, MSCE**[g], **S. Bruce Greenberg, MD**[h], **Alexander Sheldon Herbert, RT**[i], **Henri Justino, MD**[j], **Douglas Mah, MD**[k], **Mahadevappa Mahesh, PhD**[l], **Cynthia K. Rigsby, MD**[m,n], **Timothy C. Slesnick, MD**[o], **Keith J. Strauss, MSC**[p], **Sigal Trattner, PhD**[q], **Mohan N. Viswanathan, MD**[r], and **Andrew J. Einstein, MD, PhD**[s] **on behalf of the Image Gently Alliance**

[a]Department of Pediatrics, Duke University Medical Center, Durham, North Carolina (Image Gently Alliance representative)

[b]Department of Radiology, Duke University Medical Center, Durham, North Carolina (Image Gently Alliance and SPR representative)

[c]Department of Pediatric Cardiology, Children's Heart Clinic at The Children's Hospitals and Clinics of Minnesota and the Minneapolis Heart Institute, Minneapolis, Minnesota (SCCT representative)

[d]Department of Medicine, Warren Alpert Medical School of Brown University, Providence, Rhode Island (ASNC representative)

[e]Department of Pediatrics, Nationwide Children's Hospital, Ohio State University, Columbus, Ohio (ACC representative)

[f]Department of Medicine, University of Ottawa Heart Institute, Ottawa, Ontario, Canada (SNMMI representative)

[g]Department of Pediatrics, Children's Hospital of Philadelphia, Perelman School of Medicine at the University of Pennsylvania, Philadelphia, Pennsylvania (Image Gently Alliance representative)

[h]Department of Radiology, Arkansas Children's Hospital, Little Rock, Arkansas (NASCI representative)

[i]Department of Radiology, New York-Presbyterian Morgan Stanley Children's Hospital, New York, New York (ASRT representative)

[j]Department of Pediatrics, Texas Children's Hospital, Baylor College of Medicine, Houston, Texas (SCAI representative)

ADDRESS FOR CORRESPONDENCE: Dr. Andrew J. Einstein, Columbia University Medical Center, 622 West 168th Street PH 10-203, New York, New York 10032. andrew.einstein@columbia.edu.

All other authors have reported that they have no relationships relevant to the contents of this paper to disclose.

[k]Department of Pediatrics, Boston Children's Hospital, Boston, Massachusetts (PACES representative)

[l]Department of Radiology and Radiological Science, The Johns Hopkins University School of Medicine, Baltimore, Maryland (AAPM representative)

[m]Department of Medical Imaging, Ann & Robert H. Lurie Children's Hospital of Chicago, Chicago, Illinois

[n]Department of Radiology, Northwestern University Feinberg School of Medicine, Chicago, Illinois (ACR representative)

[o]Department of Pediatrics, Children's Healthcare of Atlanta, Emory University School of Medicine, Atlanta, Georgia (AAP representative)

[p]Department of Radiology, Cincinnati Children's Hospital Medical Center, Cincinnati, Ohio (Image Gently Alliance Representative)

[q]Division of Cardiology, Department of Medicine, Columbia University Medical Center, New York, New York (Image Gently Alliance representative)

[r]Department of Internal Medicine, Stanford University, Stanford, California (HRS representative)

[s]Division of Cardiology, Department of Medicine, and Department of Radiology, Columbia University Medical Center and New York-Presbyterian Hospital, New York, New York (Image Gently Alliance representative)

Abstract

There is a need for consensus recommendations for ionizing radiation dose optimization during multimodality medical imaging in children with congenital and acquired heart disease (CAHD). These children often have complex diseases and may be exposed to a relatively high cumulative burden of ionizing radiation from medical imaging procedures, including cardiac computed tomography, nuclear cardiology studies, and fluoroscopically guided diagnostic and interventional catheterization and electrophysiology procedures. Although these imaging procedures are all essential to the care of children with CAHD and have contributed to meaningfully improved outcomes in these patients, exposure to ionizing radiation is associated with potential risks, including an increased lifetime attributable risk of cancer. The goal of these recommendations is to encourage informed imaging to achieve appropriate study quality at the lowest achievable dose. Other strategies to improve care include a patient-centered approach to imaging, emphasizing education and informed decision making and programmatic approaches to ensure appropriate dose monitoring. Looking ahead, there is a need for standardization of dose metrics across imaging modalities, so as to encourage comparative effectiveness studies across the spectrum of CAHD in children.

Keywords

cardiovascular imaging; cardiovascular interventions; children; ionizing radiation; radiation safety

Children with congenital and acquired heart disease (CAHD) represent a vulnerable patient population, many of whom will require life-long medical care. In these children, cardiac imaging using ionizing radiation is essential for accurate diagnosis and safe intervention. At the same time, exposure to ionizing radiation introduces radiation-related risks, including the potential development of cancer (1–3). Recent epidemiological studies evaluating childhood exposure to computed tomography (CT) scans have asserted an increased lifetime relative risk of cancer (4–6). However, these and other reports have also highlighted the complexities and uncertainty associated with estimating long-term risks associated with the low-dose ionizing radiation exposures that are typically seen with medical imaging procedures, engendering continued debate (7, 8). There continues to be a great deal of misunderstanding among the general public regarding radiation risks, often promulgated by the media (9), as well as regarding which modalities utilize ionizing radiation (10–16).

Despite uncertainty regarding the magnitude of risk, if any, there is universal agreement that every effort should be made to keep radiation exposure from medical imaging as low as reasonably achievable so long as diagnostic integrity and procedural safety are not compromised (2). A key strategy for radiation safety in cardiology is education, often through informed discussions of the benefits and potential risks of a given procedure among patients, parents and other caregivers, and clinical and imaging health care providers (17). The education of providers—both those ordering studies and those performing and interpreting these studies—is critical. Principles of radiation protection include justification, to ensure that an imaging procedure is clinically necessary and appropriate and optimization, to ensure that radiation exposure is the appropriate amount and kept as low as reasonably achievable. Optimization does not imply dose reduction at any cost; misuse occurs both with too much and too little radiation dose. Optimization in medicine is “best described as management of the radiation dose to the patient to be commensurate with the medical purpose” (18). The overarching aim of optimization within the medical context is to ensure that “the level of protection should be the best for the prevailing circumstances, maximizing the margin of benefit over harm” (18). The purpose of this scientific statement is to provide expert consensus recommendations for optimization of medical imaging procedures commonly performed in children with CAHD, including cardiac CT, nuclear cardiology studies, and fluoroscopically guided diagnostic and interventional catheterization and electrophysiology procedures.

These recommendations specifically focus on optimization approaches that, when properly implemented, will improve the radiation safety profile for children with heart disease, without compromising the diagnostic information provided by these valuable studies or other aspects of procedural safety. They are provided in the context of unique considerations in the care of children with CAHD (19), including the reality that performance of diagnostic and image-guided interventional care may differ among centers of pediatric focus, including children’s hospitals and university practices, and community practices.

CHILDHOOD HEART DISEASE, IONIZING RADIATION, AND ASSOCIATED RISKS

Congenital heart disease is the most common birth defect, affecting an estimated 1 million children living in the United States (20, 21). Cardiomyopathies and other forms of acquired heart disease affect an additional 1 of every 100,000 children and adolescents annually (22). Children with CAHD often require complex medical care. They frequently have prolonged hospital stays and many require staged or repeated surgical interventions. The complexity of their care dictates that they are often exposed to a relatively high number of diagnostic medical imaging procedures involving ionizing radiation. In addition to diagnostic imaging, image-guided interventional procedures have become increasingly important in their care, with a substantial net increase in the average number of exposures per patient over the past 2 decades (23). Although these diagnostic and therapeutic procedures have contributed greatly to improved outcomes in children with CAHD, several studies have demonstrated that these children can be exposed to relatively high cumulative doses of ionizing radiation (24, 25).

There is increasing awareness of the potential harmful effects of exposure to ionizing radiation from imaging procedures (1–3). Relatively high doses of ionizing radiation can cause tissue reactions (formerly referred to as deterministic effects) such as skin ulceration and hair loss, whereas stochastic effects such as cancer have been attributed to even relatively low doses. Tissue reactions result from radiation-induced cell death or damage and are only very rarely seen in children because individual procedural doses typically do not exceed threshold levels. By contrast, for stochastic effects, most expert panels have opined that the existing data best support a linear, no-threshold relationship to ionizing radiation dose, as a basis for radiation protection. Stochastic effects are due to ionizing radiation–induced mutations and occur more commonly in rapidly dividing cells and in higher cancer risk organ and tissue structures such as breast, bone marrow, stomach, colon, and lung tissues (2). Although mutations occur at the time of exposure, there is often a substantial time lag between exposure and onset of solid cancers which may be diagnosed decades later. Because children have more rapidly dividing cells within organs and tissues, and because there is typically a longer anticipated lifespan following exposure during which cancer can develop, exposures that occur at younger ages are associated with increased risk (1). Similarly, females are at increased risk due in large part to their increased risk of breast cancers. With increasing recognition of the lifetime risks associated with ionizing radiation exposure, and acknowledging the vital diagnostic and therapeutic role of medical imaging procedures that use ionizing radiation, it is critical to optimize these procedures so as to achieve sufficient diagnostic yield at reduced radiation doses when possible.

OPTIMIZATION AND JUSTIFICATION

The principles of justification and optimization form the backbone of medical imaging dose management recommendations (26). Justification, when discussed in the context of the individual patient, suggests that a medical procedure is both appropriately indicated and that the anticipated clinical benefits exceed all anticipated risks, including radiation risk. In adult cardiology, where there are established appropriate use criteria (27–29), a significant

percentage (from ~5% to >45%, depending on the study and imaging modality) of cardiac imaging studies has questionable justification (30–34). Similar appropriate use criteria have not been developed for pediatric cardiac imaging procedures that utilize ionizing radiation, and it is unclear what proportion of medical imaging procedures would generally be considered justified in these patients. Justification is an indispensable part of radiation protection in children, on the basis of the ethical principles of nonmaleficence and beneficence.

As defined in the preceding text, optimization entails that the radiation dose to the patient is suitable for the intended medical purpose, and radiation that is clinically unnecessary or unproductive is avoided (2). Regardless of the imaging modality, optimization strategies almost always vary depending on the patient size or body habitus. Strategies for dose optimization in adults typically cannot simply be applied to children. For practitioners engaged in pediatric medical imaging procedures that use ionizing radiation, it is necessary to understand the unique needs of children and the challenges of optimized imaging across the spectrum of pediatric patients from the premature neonate to the adult-sized adolescent.

DOSE METRICS

A variety of metrics are used to quantify the radiation burden of cardiovascular procedures. These include both general terminology (2) and modality-specific metrics (35). One or more dose metrics should be recorded for all cardiovascular imaging procedures in children with CAHD.

GENERAL METRICS

Ionizing radiation deposits energy in the human body, which creates charged particles (ionized tissue molecules) that have the potential to cause biological damage. The absorbed dose is an estimate of the energy deposited. Because less energy is carried by a fluoroscopic x-ray beam to deeper layers of tissue due to large deposits of energy in the superficial layers (attenuation), one should designate the location of a specified absorbed dose, for example, absorbed dose to a whole organ or tissue, skin entrance, midline, or exit plane. Today, absorbed dose is expressed in Système International units of grays (Gy, mGy, mGy, and so on), whereas, historically, it was expressed in units of rads or mrads, where 1 mGy = 100 mrad. A related concept is the equivalent dose, which weights absorbed dose to reflect the ability of the specific type of radiation to cause biological damage. For x-rays and gamma-rays, which are the types of radiation used in imaging children with CAHD, this weighting factor is 1, so absorbed and equivalent doses take equal values. However, equivalent dose is expressed in Système International units of sieverts (Sv, mSv, and so on), not grays. The historical unit was the rem, where 1 mSv = 100 mrem (2).

Another general metric, used across modalities and facilitating comparisons between modalities, is the effective dose. Effective dose is a whole-body quantity representing a sum of organ equivalent doses, each weighted by a tissue weighting factor that reflects the radiation detriment from stochastic effects for that organ. These tissue weighting factors are prescribed in international standards and derive from synthesis of the extant worldwide radio-epidemiological data (2). Current tissue weighting factors for effective dose are age-

and sex-averaged values, thus posing a limitation in characterizing a patient-specific stochastic radiation risk on the basis of effective dose, especially in children. Effective dose enables comparisons between exposure scenarios where different parts of the body receive different exposures, and is also expressed in units of sieverts. A dose expressed in units of sieverts could be either an effective or equivalent dose, and thus care should be taken to specify which quantity is being described. For example, if an effective dose is incorrectly interpreted as an equivalent dose, the dose to directly irradiated organs and their potential risk from a diagnostic examination could be significantly underestimated.

CT METRICS

Several related CT dose index quantities exist, which are calculated from dosimetric measurements performed in a cylindrical Plexiglas phantom (35). These include the volume CT dose index ($CTDI_{vol}$), the dose–length product (DLP), and the size-specific dose estimate (SSDE). $CTDI_{vol}$, reported by current CT scanners, is calculated from both peripheral and central dosimetric measurements performed in a cylindrical phantom, as well as the pitch for a helical scan. It can be performed using a phantom of either 32 or 16 cm in diameter. DLP, also reported on current scanners, is calculated as $CTDI_{vol}$ multiplied by the scan length, and it reflects a total radiation burden from a scan, not just a dose at a single location. SSDE (36), a recently introduced CT dose metric not yet reported by CT scanners, normalizes $CTDI_{vol}$ to reflect patient size (effective diameter) (36). Published conversion factors (36) are multiplied by the displayed $CTDI_{vol}$ to calculate the SSDE. The size of the patient and size of the phantom used to calculate the displayed $CTDI_{vol}$, are required to identify the correct published conversion factor for an individual patient. Conversion factors to estimate the effective dose from DLP in children are available (Tables 1 and 2), but SSDE cannot be converted to DLP (36) or effective dose.

A consensus on a standard for radiation dose reporting for cardiovascular CT in pediatric patients has not been established, although California law requires physicians to record $CTDI_{vol}$ and DLP for all CT scans (44). Nonetheless, when $CTDI_{vol}$, DLP, or SSDE is reported, the size of the phantom used in its determination should also be reported. If an effective dose estimate is calculated, the cardiac- or chest-specific conversion factor used in its estimation should be reported. Methodological specification is especially important in children because CT dose estimates can vary several fold depending on the method of calculation used, and dose comparisons between modalities should reflect similar adjustments to enable a valid comparison.

NUCLEAR MEDICINE METRICS

The activity of a radiopharmaceutical is the average number of nuclear decays per unit time. The Système International unit of activity is the Becquerel (Bq), which is used to refer to 1 decay per second. In the United States, the traditional unit of curies (Ci) is more commonly used, where $1\ Ci = 3.7 \times 10^{10}$ Bq. For a given activity of a radiopharmaceutical, effective dose (as well as organ absorbed doses) can be estimated by multiplying the activity by a dose coefficient, determined on the basis of biokinetic models. Dose coefficients for many radiopharmaceuticals and children of a range of ages, can be found in publications of the International Commission on Radiological Protection (45–48) and the Society of Nuclear

Medicine and Molecular Imaging (49), as well as in radiopharmaceutical package inserts. Pediatric dose coefficients for commonly used cardiac radiopharmaceuticals are compiled in Table 3.

FLUOROSCOPY METRICS

Interventional fluoroscopic equipment used in the catheterization lab displays cumulative air kerma ($K_{a,r}$) in units of mGy from the procedure at an interventional reference point designed to approximate the entrance skin plane of an adult patient. This dose index can be used by a qualified medical physicist to estimate the skin dose to the patch of skin of the patient that received the largest radiation dose during the examination: the peak skin dose, which is typically less than the cumulative air kerma. Peak skin dose is an indicator of the likelihood that the patient will develop a tissue reaction as a result of the examination. This risk is greater in large adults than small children for whom a lower dose is required to achieve adequate image quality. Prototypes of real time feedback to the operator of the increasing peak skin dose during the examination are available on a limited number of vendors' equipment. When biplane interventional equipment is used for pediatric patients, the $K_{a,r}$ from the frontal and lateral planes should ideally not be added, given that each plane exposes a different area of skin.

These same fluoroscopes also display the kerma–area product (KAP) or dose–area product to the patient from the examination. The KAP is the product of the air kerma and the cross-sectional area of the x-ray beam. This quantity is constant at all distances from the source because the former falls, whereas the latter rises, both as the square of distance from the x-ray source. KAP is commonly measured using a special meter designed for this purpose that is built into the fluoroscopy unit, near the collimator. Analogously to DLP for CT, KAP reflects not just the kerma (dose) at the skin surface as does $K_{a,r}$, but also the area of tissue that is irradiated, and as such, it better reflects the stochastic risk from a procedure than does $K_{a,r}$. Thus, KAP is generally used as a surrogate of stochastic risk, whereas $K_{a,r}$ is used as a marker of deterministic risk, that is, risk of a tissue reaction. Although Monte Carlo simulations have been performed for anteroposterior and lateral exposures to relate $K_{a,r}$ and KAP to organ and effective dose in children (50), conversion factors enabling simple estimation of organ and effective doses from commonly performed pediatric cardiac fluoroscopic procedures have not yet been determined.

OPTIMIZATION STRATEGIES FOR CARDIAC COMPUTED TOMOGRAPHY

Cardiovascular CT is an increasingly common modality in children with CAHD (51–53). Modern cardiovascular multidetector CT (MDCT) scanner technology delivers detailed cardiac morphological imaging at the fast heart rates of children (51), reduces the need for sedation compared with magnetic resonance (MR) imaging (52) or cardiac catheterization, and can be performed at effective doses of <1 mSv (54–56). Guidelines for advanced noninvasive cardiovascular imaging in children with CAHD do not include recommendations regarding cardiovascular CT (57), although cardiac imagers must be proficient in radiation dose management strategies to mitigate potential radiation risks for patients with cardiovascular disorders (58, 59). In addition, current variability (60) of

radiation dose for cardiovascular CT in pediatric cardiovascular disorders could be reduced by universal application of radiation dose optimization techniques.

Every cardiovascular CT scan performed in a patient with cardiovascular disorders should be tailored to the individual patient and clinical indication. This informed and individualized scan performance for pediatric CT can be separated into the 2 categories of patient preparation and scan acquisition. Table 4 and the Central Illustration summarize optimization strategies for patient preparation and scan performance.

Patient preparation recommendations for dose optimization in cardiovascular CT include consultation with the referring cardiologist and surgeon when necessary. Heart rate–lowering medications, including beta-blockers, calcium channel blockers, and phenylephrine, should be considered for high-resolution coronary artery imaging (61–63). The lowest radiation dose will be delivered with a slower and steady heart rate for electrocardiogram (ECG)-gated/triggered scans (64). For gated studies, heart rate–lowering medication will often allow use of a narrow acquisition window, that is, x-ray exposure during a shorter portion of the cardiac cycle. With faster acquisition (e.g., dual source or wide detector array scanning), nongated studies may give adequate evaluation of extracardiac structures such as the aorta and pulmonary veins at a lower radiation dose (65–68). Sedation and/or anesthesia for suspended respiration in patients unable to cooperate may be needed when a protocol requiring several heart beats is used and patient motion may affect image quality. Examples include ECG-gated functional imaging or high-resolution coronary artery imaging at fast heart rates. Sedation and/or anesthesia can reduce overall heat rate and heart rate variability due to patient agitation. Rarely, pacemaker rate and mode should be adjusted for optimal imaging (69). Iodinated intravenous (IV) contrast media administration (including iodine concentration, dose, rate of administration, gauge, and location of IV access) should be planned to opacify all structures of interest. Optimally, all necessary information should be obtained in a single scan acquisition. For example, a 2-phase contrast injection can be used to opacify the right and left heart simultaneously, or a 2-phase contrast injection separated by a pause can be used to provide venous and arterial opacification in the same scan (58).

Scanner-based optimization approaches include limiting the scan range to the anatomy requiring evaluation. The patient should be centered within the gantry (70). Scanner parameters such as tube current (mA) and tube potential (kVp) should be adjusted to patient size. Lower tube potential settings (e.g., 70 and 80 kVp for most children; 80 or 100 kVp in adolescents and small adults) should generally be selected (71, 72). Technique should also be adjusted to yield acceptable image quality that is tailored to the clinical indication. For example, a CT scan performed for evaluation of aortic coarctation after balloon angioplasty and stent placement typically can be fully diagnostic at a lower radiation dose than a scan performed for evaluation of coronary arterial anatomy. The scan mode chosen should provide the diagnostic image quality at the lowest practical radiation dose. Prospective ECG triggering rather than retrospective ECG gating should be used when possible. Retrospective gating, which results in a relatively higher radiation dose, should be reserved for highly irregular heart rates (73, 74). ECG-gated tube current modulation should typically be used for functional imaging. This limits the fully irradiated portion of the cardiac cycle to a narrow window and gives a reduced dose (typically 20%) through the remainder of the

cardiac cycle (75). The narrowest temporal acquisition window possible should be used for coronary imaging. For coronary artery origin and location, a narrow window will often provide adequate visualization (76), reserving a widened window for high resolution coronary imaging at high heart rates (76, 77). Use of automated tube current (78) and tube potential (79) algorithms should be considered (78, 80). Iterative reconstruction should be used on all scans (81, 82). Collaboration among qualified cardiac imaging physicians, technologists, and medical physicists, as well as the CT vendor's product specialists should lead to more effective protocols. By virtue of using a combination of approaches, cardiac CT with good diagnostic image quality can be obtained using low radiation doses (Figure 1), and even without the most advanced technology.

OPTIMIZATION STRATEGIES FOR NUCLEAR CARDIAC IMAGING

Not only are children more sensitive to the effects of ionizing radiation than are adults, but also the radiation dose from a given activity of a radiopharmaceutical is greater for children than for adults. For example (Table 3), a 10 mCi dose of 99mTc sestamibi administered at exercise has an associated effective dose of 2.9 mSv in an adult, 3.7 mSv in a 15-year-old, 5.9 mSv in a 10-year-old, 8.5 mSv in a 5-year-old, and 16.7 mSv in a 1-year-old child (45, 47, 83). This variability underscores the importance of radiation dose optimization when a nuclear cardiology procedure is clinically determined to be the right test for a child.

Several approaches exist that can and should be used for dose optimization of nuclear cardiology procedures in children (Table 5, Central Illustration). Most nuclear cardiac studies in children are single-photon emission computed tomography (SPECT) myocardial perfusion studies. Thallium-201, which has a long half-life (3 days) and relatively high radiation dose, should be avoided. In general, a stress-first/stress-only approach using a technetium-99m–based radiopharmaceutical (sestamibi or tetrofosmin) should be performed. Here, stress testing and stress imaging is performed first, with stress images reviewed by an attending nuclear cardiology physician before any rest imaging, and rest imaging (with its attendant radiation dose) omitted if stress perfusion and left ventricular function, wall motion, and size are all normal (84). Multiple-position imaging, which for most cameras entails both supine and prone imaging, has been demonstrated to increase the normalcy rate of stress imaging and thus can increase the proportion of children not requiring subsequent rest imaging (85). In children, when rest imaging is needed, it should be performed on a later day than stress imaging, using the same administered activity (mCi), because same-day stress–rest myocardial perfusion imaging requires a rest activity of 3 to 4 times the stress dose to minimize the effect of residual stress activity on the rest study ("shine-through artifact") (86).

Determination of administered activity should be tailored to the patient's size. North American consensus guidelines suggest Tc-99m sestamibi or tetrofosmin activity for children of 0.15 mCi/kg for the first scan in a given day, with a minimum of 2 mCi and a maximum of 10 mCi (87). These guidelines do not recommend activities for other radio-pharmaceutials used in pediatric nuclear cardiology. However, several additional formulas exist (Table 6) that can be used to adjust the dose from a standard adult activity, on the basis of a child's age, weight, or body surface area. The recommended pediatric administered

activity often varies widely among these formulas. For example, for an 11-year-old, 75-lb, 56-inch child undergoing exercise testing with Tc-99m sestamibi or tetrofosmin for evaluation of an anomalous coronary artery, North American consensus guidelines suggest an activity of 5.1 mCi, Clark's rule suggests an activity of 5.0 mCi, Young's rule, 4.8 mCi, Webster's formula, 6.7 mCi, a body-surface-area–based approach, 6.7 mCi, and the European Association of Nuclear Medicine (EANM) Dosage Card (88), 8.8 to 13.1 mCi. In practice, it may be useful to calculate recommended activity using several of these methods and then heuristically select within the range determined.

When possible, technological advances in instrumentation—such as a high-efficiency cadmium-zinc-telluride camera or positron emission tomography (PET), or image reconstruction software incorporating iterative reconstruction, resolution recovery, and noise reduction—should be used to reduce administered activity and hence radiation dose. Such methodology can result in outstanding image quality (Figure 2) using a lower administered activity, generally no more than 5 mCi of 99mTc, than that from any formula. It is desirable to obtain at least 1 million left ventricular region counts for each scan, with reconstruction filtering lowered to preserve resolution of the smaller heart walls (9).

Because Tc-99m–based perfusion agents are "sticky" with adsorption of some radiopharmaceutical to the syringe and stopcock, when using low Tc-99m activity one should be careful to flush the syringe containing Tc-99m with saline after peak-exercise administration and inject this flush into the patient; to measure residual post-injection activity in the syringe and stopcock; and to prolong imaging time if net received activity is significantly lower than anticipated. Although overly low activity (e.g., <2 mCi) is not recommended a priori, it need not result in an uninterpretable study that might otherwise need to be repeated.

In centers where PET myocardial perfusion imaging is available, it may be preferred versus SPECT due to lower radiation dose, higher spatial resolution, and higher accuracy. However, few centers perform exercise PET stress testing, and pharmacological vasodilator stress may not be adequate in simulating the effects of exercise for many children requiring myocardial perfusion imaging, for example, those with anomalous coronary arteries. If x-ray CT attenuation correction is used, the lowest possible tube current should be used to maintain accurate attenuation correction only, that is, diagnostic-quality CT is not required. The CT DLP should rarely exceed 15 mGy · cm. Three-dimensional (3D) PET acquisition mode should be used if possible with body habitus–or weight-based adjustment of the injected activity to minimize radiation exposure. For example, the combined effective dose for stress and rest imaging of a 10-year-old pediatric patient weighing 75 lbs (34 kg) is (Table 3) approximately 2 mSv using 10 MBq/kg of Rb-82 or 5 MBq/kg of N-13 ammonia (48). The image reconstruction smoothing filter should be selected to optimize spatial resolution of the myocardial walls versus background noise. Stress-first imaging should be employed as described earlier in the text for SPECT, unless there is a specific request for assessment of stress/rest myocardial flow reserve, although relevant pediatric data are extremely limited.

OPTIMIZATION STRATEGIES FOR FLUOROSCOPICALLY GUIDED PROCEDURES

Fluoroscopically guided procedures, including diagnostic, interventional, and electrophysiological cardiac catheterization procedures, on average, account for more cumulative ionizing radiation to children with CAHD than all other medical imaging modalities combined (24, 25, 89, 90). Radiation doses for individual procedures can vary widely depending on the size of the patient, complexity of the procedure, hardware and configuration of the fluoroscope, and the optimization practices of the proceduralist during the examination.

Dose reduction strategies during fluoroscopy can be classified into 2 broad, but overlapping, categories: 1) aspects of the imaging equipment's hardware/configuration that must be selected to support pediatric imaging at the time the system is selected, installed, and/or configured; and 2) operator-dependent approaches to imaging that are often manipulated immediately before or during the procedure by the proceduralist or staff. Recommendations for management of patient dose while maintaining diagnostic quality images focused on hardware, configuration, and operator-dependent techniques are provided in Tables 7 to 9, respectively. These recommendations should be considered as guidelines rather than strict rules. Every imaging scenario requires an individualized approach, and dose management should never compromise image quality to the extent that diagnostic accuracy and/or procedural safety are adversely impacted.

HARDWARE AND CONFIGURATION

No currently marketed fluoroscope is designed solely for pediatric use. "Out of the box" new fluoroscopes are typically not configured for the unique challenges of pediatric imaging. Using a fluoroscope configured for adult patients on a child or infant can result in ionizing radiation doses that are orders of magnitude higher than needed (91–93). For these reasons, optimization of the fluoroscopic hardware and its configuration is critical. The process of hardware and software configuration should involve close collaboration among the physicians performing these procedures, the technologists, technicians, and physician extenders in the catheterization laboratory, the fluoroscope's design engineers and qualified medical physicists (94, 95).

OPERATOR-DEPENDENT TECHNIQUES

Continuously managing doses during a complex imaging procedure requires an understanding of the capabilities and limitations of the fluoroscope, establishing good practice habits, and using all the appropriate features of the imaging equipment (96). When effectively implemented, these approaches can reduce both the radiation dose per image and the number of images created during a procedure without compromising the quality of the study (Figure 3) (92).

In addition to the recommendations provided in Tables 7 to 9, further explanation is required regarding the use of anti-scatter grids (Figure 4). These grids are beneficial when there is significant scattered radiation. However, when scatter is reduced (i.e., in smaller patients),

anti-scatter grids continue to attenuate some of the unscattered x-rays leading autoexposure controls to increase radiation output of the system, thereby contributing to increased dose to the patient with little benefit (97). Although the operator's tolerance for reduced contrast in the image (subjective) should determine when the grid is removed, for ease of implementation, we have provided a consensus recommendation for removal in children <20 kg. This is subject to reappraisal as newer technologies emerge and may require ongoing discussion with equipment vendors. Providers should note that if other imaging parameters are left unaltered, then removing the grid will always reduce the dose. In larger children or adults, this is detrimental to image quality. Therefore, individual practices may prefer to define the specific body habitus limits at which they feel image quality is sufficiently degraded to warrant using an anti-scatter grid.

The air gap technique (Figure 5) is an alternate approach designed to limit the effects of scatter radiation on image quality without the dose penalty associated with an anti-scatter grid. With this technique the anti-scatter grid is removed, and the image receptor is moved approximately 15 cm from the patient, thereby creating an air gap. The geometry of the air gap causes most of the obliquely scattered x-rays emitted from the patient to "miss" the image receptor, whereas all the unscattered x-rays reach the image receptor. Without the grid in place, there is an increased dose rate to the image receptor, and the automatic exposure control system will respond by decreasing the dose rate delivered to the patient (98). The increased receptor height also creates geometric magnification in the image. At 15 cm, this approximates a 1-step increase in electronic magnification, and users can maximize dose reductions by reducing the electronic magnification. However, as geometric magnification grows with increased air gap, perceptible image blur results in most cardiac systems with focal spots larger than 0.3 mm. Given the complexity of using geometric magnification properly, we recommend that practices work with qualified medical physicists to evaluate the impact of the air gap technique on the dose–image quality relationship with their fluoroscope. It is important to note that the air gap technique should not be used when the anti-scatter grid is in place. This redundancy needlessly increases overall dose to the patient due to auto-exposure control response to reduced signal intensity at the receptor.

USE OF FLUOROSCOPY DURING ELECTROPHYSIOLOGY PROCEDURES

Advances in imaging techniques, specifically, 3D electroanatomic mapping (EAM) systems, have significantly reduced the use of fluoroscopy within the electrophysiology lab. These mapping systems, such as CARTO (Biosense Webster, South Diamond Bar, California) and Nav-X (St. Jude Medical, St. Paul, Minnesota), allow for the creation of 3D shells of intracardiac chambers and vessels, over which catheters can be visualized without the use of radiation. As EAM tools have advanced, the ability to perform safe and effective ablations using minimal radiation has been demonstrated in numerous studies (99–104). For these reasons, we encourage the use of 3D EAM during electrophysiology procedures in children.

However, as electrophysiologists strive to perform zero-fluoroscopy studies, there is continued acknowledgment that fluoroscopy is still necessary for specific aspects of an electrophysiology procedure. This includes maneuvering long sheaths that cannot be seen on an EAM system and trans-septal needle punctures, although the latter could be addressed

with intracardiac echocardiography and operator familiarity with intracardiac images. In addition, the financial costs of additional tools to allow nonfluoroscopic trans-septals and the need for an additional venous sheath should be weighed against the amount of fluoroscopy saved (100). Lastly, some EAM systems, such as the CARTO UniVue platform, actually encourage a limited amount of fluoroscopy. Spot fluoroscopic pictures can be stored and used as background images on which electroanatomic shells can be superimposed. As such, the use of nonfluoroscopic imaging tools should go hand in hand with radiation reduction techniques. Even if the fluoroscopy time is minimal, electrophysiologists should not neglect the basic tenets of radiation reduction, as outlined in Tables 7 to 9. Moreover, consistent with our earlier recommendations, optimization of the fluoroscopic hardware and its configuration is important for electrophysiology procedures, just as it is for any procedure involving fluoroscopic guidance. Relative to cardiac catheterization procedures, electrophysiology procedures can potentially be safely performed using lower frame rates as well as lower a dose per frame for both acquisition and fluoroscopy imaging (105). Providers should work with the fluoroscope's design engineers and/or qualified medical physicists to develop imaging protocols that meet the specific needs of the electrophysiology laboratory.

PROGRAMMATIC APPROACHES TO ENSURE SUSTAINED BEST PRACTICES

Programmatic quality controls, including checklists and dose monitoring practices, can help sustain program-wide dose reduction efforts. These approaches track performance, motivate team members, and facilitate sustained, high performance. Several studies have demonstrated the benefits of implementing systematic approaches such as these (106, 107). Resources are available to guide institutions with implementation of quality improvement initiatives, including the Society for Cardiovascular Angiography and Interventions "Pediatric Radiation Safety Quality Improvement Toolkit" (108). The qualified medical physicist who performs periodic equipment compliance testing should be able to set up simple periodic tests to track the constancy of image quality and patient radiation dose rates of the x-ray equipment in the catheterization laboratory.

THE IMPORTANCE OF PATIENT/CAREGIVER-CENTERED IMAGING

Public, patient, and caregiver (e.g., parent) knowledge of the risks of ionizing radiation is often relatively limited; some patients and caregivers are unaware of the potential for harmful effects, whereas others, sometimes heavily influenced by media misrepresentation, perceive risks far greater than those that actually exist (9, 10, 109). When surveyed, parents of children undergoing medical imaging procedures overwhelmingly state that they prefer to be informed of risks (10, 110). Moreover, communication of risk is a fundamental responsibility of professionalism, including patient autonomy (111, 112). We encourage involving families in the decision-making process by communicating anticipated risks and benefits of the planned procedure, including those associated with radiation exposure when these are anticipated to be sufficiently high (113). The method and extent of communication can be tailored to the risks and benefits of any given imaging scenario, such as potential cognitive deficits from general anesthesia (114) used for MR evaluation in young children, or IV contrast media for either CT or MR (115, 116). An offer to provide written or

electronic materials may suffice for lower-dose procedures, whereas for procedures involving higher doses, direct verbal communication, with or without formal written consent, may be more appropriate. Radiation dose thresholds that dictate the level of discussion have been previously recommended for adult cardiac imaging. These recommendations, provided by an expert panel sponsored by the National Institutes of Health–National Heart, Lung, and Blood Institute/National Cancer Institute, specify that when there is an anticipated procedural effective dose of ≤3 mSv, the procedure is of very low risk and not warranting extensive discussion or written informed consent. By contrast, an anticipated effective dose of ≥20 mSv is considered at a level requiring either formal discussion or written informed consent (117). It is beyond the scope of this paper to recommend specific dose cutpoints for pediatric cardiac imaging; however, doses of >20 mSv have been reported for some pediatric cardiac imaging procedures, and these adult guidelines may be useful as a frame of reference (24, 92). Finally, it is necessary to acknowledge the importance of multidisciplinary communication, including the referring physician, imaging physician, and other members of the care team (118). This is paramount to ensure that the procedure is performed for appropriate indications with good understanding of the risks and benefits (113, 119).

INSTITUTING A DOSE MONITORING PROGRAM

Inherent in the accountability for ionizing radiation dose management across all ages and for any imaging specialty is that of auditing of clinical practice and modification of practice on the basis of the results as necessary (120). For imaging, this has been referred to as dose tracking or dose monitoring and has recently become a required component of practice accreditation for CT and nuclear medicine, as outlined in The Joint Commission's 2015 document Diagnostic Imaging Requirements (121). The major goal of a dose monitoring program is to improve individual patient care, as well as the performance across a population of patients within a practice or institution. The primary components of a dose monitoring program consist of: 1) definition of dose metrics to monitor; 2) access to these metrics across different equipment vendors within modalities, as well as between different modalities to enable consistent structured reporting; 3) quality and accuracy of the dose metrics, including the need for harmonious nomenclature for the examination (affording comparison within and between practices and over time); 4) clear analytics to summarize effectively the large amount of data that can be available; and 5) data access and display that are both user friendly and include appropriate security, encryption, and backup. A dose monitoring program is the responsibility of any imaging team and includes physicians and their delegates, including technologists and medical physicists with a heavy dependency on information technology specialists and administration.

Information to monitor includes protocol-specific dose metrics that can serve in the establishment of standards of performance (also known as diagnostic reference levels [DRLs]) for the practice, as well as comparison to existing benchmarks, for example, through public registries such as the Dose Index Registry for x-ray CT (122) and the ImageGuide Registry for nuclear cardiology procedures (123). Methods should be established for identifying dose values outside of the defined reference range (e.g., between first and third quartiles) and for assessing system variability and trends over time, as well as

discrepancies between the protocol definitions and protocols performed in clinical practice. One important consideration is whether past radiation history should impact decisions for current or future radiation use for an individual patient (15). Other challenges include large amounts of data to analyze, what to record, where to report dose metrics (e.g., patient report, PACS [picture archiving and communication system], other archive), inaccurate dose metrology (patient dose estimations), current lack of standardized DRLs (and thresholds for corrective actions), especially using fluoroscopy in the interventional suite, unclear frequency of interrogation, and establishment of authoritative program governance.

RESEARCH NEEDS AND FUTURE DIRECTIONS

Although there are many unmet research needs in terms of improving radiation safety in children with CAHD, several overarching objectives could serve as a framework to accelerate future advances. First, there is a critical need for dose metrics that are standardized and patient-centered, across the spectrum of imaging modalities. The current status quo, with differing metrics preferred depending on the imaging modality, can be confusing for patients and providers, and also poses challenges for comparative effectiveness evaluation. The ideal dose metric should endeavor to assess organ dose, because organ absorbed doses can be more readily compared across the wide spectrum of patient sizes in pediatrics and because organ absorbed doses are also the preferred metric for quantification of stochastic risks (the major radiation-related concern in children). To this end, there is a need to develop pediatric conversion factors to facilitate efficient conversion from standard modality-specific dose metrics (e.g., DLP, SSDE, KAP, and $K_{a,r}$) to metrics that reflect organ absorbed doses as well as effective dose.

Standardization of dose metrics would also encourage our second identified overarching research need: a need for comprehensive (e.g., risk informed) comparative effectiveness evaluation across the spectrum of medical imaging in children with CAHD. Radiation exposure is one factor among many that can be assessed and compared between testing strategies in such a context. In adult cardiology, several completed and on-going randomized comparative effectiveness trials have evaluated specific clinical scenarios in which different imaging-based management strategies are considered. These trials are often particularly high yield as even negative trials can reduce the use of ionizing radiation and decrease population exposure. Examples of such studies include the DIAD (Detection of Ischemia in Asymptomatic Diabetics) trial, studying screening nuclear stress testing in asymptomatic diabetic patients (124), the PROMISE (Prospective Multicenter Imaging Study for Evaluation of Chest Pain) study, comparing initial anatomic imaging versus functional testing strategies in patients with new symptoms suggestive of coronary artery disease (125), the SCOTHEART (Scottish Computed Tomography of the Heart) trial, assessing the effect of added coronary CT angiography in patients with suspected angina (126), and the PARR-2 (PET and the Recovery Following Revascularization-2) trial of standard versus PET-assisted management strategies in patients with left ventricular dysfunction being considered for coronary revascularization (127). Similar trials should be considered in children with CAHD, for example, to consider accurate risks and benefits of screening cardiac catheterization procedures in single-ventricle patients or optimal modalities for coronary imaging (e.g., after arterial switch operations, in patients with Kawasaki disease, or

anomalous coronary arteries). Registry- or trial-based comparative effectiveness evaluations contribute critical evidence that can be used to guide consensus guidelines focused on study justification or the development of appropriate use criteria.

Finally, there is a need to evaluate the relative merits of cumulative dose monitoring in children. Patient passport models have been advocated by some as a means to monitor cumulative dose. Benefits include enhanced patient and provider awareness, and improved understanding of the long-term consequences of cumulative exposures. However, opponents to this position argue that there is currently an inherent uncertainty in dose and risk estimates and that dose passports can create undue anxiety with the potential to adversely influence medical decision making in the absence of guidelines for appropriate identification and management of patients exposed to high cumulative doses (128).

CONCLUSIONS

Tables 4, 5, and 7 to 10 summarize consensus recommendations regarding strategies to optimize imaging during cardiac CT, nuclear cardiology, and fluoroscopically guided cardiac catheterization and electrophysiology procedures, respectively. These approaches are comprehensive, covering the spectrum of hardware and software features and configuration, as well as operator-dependent approaches to imaging. If broadly implemented by programs caring for children with CAHD, these recommendations could facilitate significant population-level reductions in cumulative ionizing radiation exposure while concomitantly ensuring high-quality imaging that does not compromise diagnostic integrity or procedural safety. Other measures, including a concerted effort to engage patients and caregivers in an informed decision making process related to medical imaging and efforts to develop program-wide dose monitoring procedures, are also recommended to improve patient care and to encourage informed imaging. The development of current cardiac imaging technologies has revolutionized the practice of cardiovascular medicine in children with CAHD by facilitating improved diagnosis and less-invasive intervention. It is now incumbent on the imaging community to ensure that these procedures are optimized to ensure image quality appropriate to the medical needs of the patient but at the lowest achievable dose.

Acknowledgments

Endorsed by the American College of Cardiology (ACC), American College of Radiology (ACR), American Academy of Pediatrics (AAP), American Association of Physicists in Medicine (AAPM), American Society of Nuclear Cardiology (ASNC), American Society of Radiologic Technologists (ASRT), Heart Rhythm Society (HRS), North American Society for Cardiovascular Imaging (NASCI), Pediatric and Congenital Electrophysiology Society (PACES), Society for Cardiovascular Angiography and Interventions (SCAI), Society for Cardiovascular Computed Tomography (SCCT), Society for Pediatric Radiology (SPR), and Society of Nuclear Medicine and Molecular Imaging (SNMMI). Dr. Hill has received support from grant UL1 TR001117 from the National Center for Advancing Translational Sciences; and is a consultant for Myocardia and Kowa Pharmaceuticals. Dr. Rigsby is supported by grant R01 HL115828 from the National Heart, Lung, and Blood Institute. Dr. Einstein is supported in part by grant R01 HL109711 from the National Heart, Lung, and Blood Institute. Dr. Han has received institutional research funding from Siemens Medical; and is a consultant for the core lab at Edwards Lifesciences. Dr. Armstrong is a member of the Siemens Healthcare AX Advisory Board in Pediatric Cardiology and Interventional Radiology; is a proctor for Abbott, B. Braun Interventional Systems, and Edwards Lifesciences; is a consultant for Abbott; and has received research grants from Abbott, Edwards Lifesciences, Medtronic, PFM Medical, and Gore. Dr. DeKemp has received royalty revenues from imaging technologies licensed to Jubilant DraxImage and INVIA Medical Imaging. Dr. Strauss is a member of Philips Healthcare’s medical physicist advisory board. Dr. Trattner

has received institutional research grants for other investigator-initiated studies from Philips Healthcare. Dr. Einstein has received research grants to Columbia University from GE Healthcare, Philips Healthcare, and Toshiba America Medical Systems.

ABBREVIAT IONS AND ACRONYMS

3D	3-dimensional
CAHD	congenital and acquired heart disease
CT	computed tomography
CTDIvol	volume computed tomography dose index
DLP	dose–length product
DRL	diagnostic reference level
EAM	electroanatomic mapping
ECG	electrocardiogram
IV	intravenous
KAP	kerma–area product
$K_{a,r}$	cumulative air kerma
MDCT	multidetector computed tomography
MR	magnetic resonance
PET	positron emission tomography
SSDE	size-specific dose estimate
SPECT	single-photon emission computed tomography

References

1. Committee to Assess Health Risks from Exposure to Low Levels of Ionizing Radiation; Nuclear and Radiation Studies Board. Health Risks From Exposure to Low Levels of Ionizing Radiation: BEIR VII Phase 2. Washington, DC: National Academies Press; 2006. Division on Earth and Life Studies, National Research Council of the National Academies.
2. International Commission on Radiological Protection. The 2007 Recommendations of the International Commission on Radiological Protection. ICRP publication 103. Ann ICRP. 2007; 37(2–4):1–332.
3. UNSCEAR. Effects of Ionizing Radiation. Report to the General Assembly of the United Nations, With Scientific Annexes. Vol. I. New York, NY: United Nations Scientific Committee on the Effects of Atomic Radiation; 2006.
4. Mathews JD, Forsythe AV, Brady Z, et al. Cancer risk in 680,000 people exposed to computed tomography scans in childhood or adolescence: data linkage study of 11 million Australians. BMJ. 2013; 346:f2360. [PubMed: 23694687]
5. Pearce MS, Salotti JA, Little MP, et al. Radiation exposure from CT scans in childhood and subsequent risk of leukaemia and brain tumours: a retrospective cohort study. Lancet. 2012; 380:499–505. [PubMed: 22681860]

6. Berrington de Gonzalez A, Salotti JA, McHugh K, et al. Relationship between paediatric CT scans and subsequent risk of leukaemia and brain tumours: assessment of the impact of underlying conditions. Br J Cancer. 2016; 114:388–94. [PubMed: 26882064]
7. Boice JD Jr. Radiation epidemiology and recent paediatric computed tomography studies. Ann ICRP. 2015; 44:236–48. [PubMed: 25816281]
8. Hendee WR, O'Connor MK. Radiation risks of medical imaging: separating fact from fantasy. Radiology. 2012; 264:312–21. [PubMed: 22821690]
9. Cohen MD. ALARA, image gently and CT-induced cancer. Pediatr Radiol. 2015; 45:465–70. [PubMed: 25680877]
10. Boutis K, Cogollo W, Fischer J, Freedman SB, Ben David G, Thomas KE. Parental knowledge of potential cancer risks from exposure to computed tomography. Pediatrics. 2013; 132:305–11. [PubMed: 23837174]
11. Carpeggiani C, Kraft G, Caramella D, Semelka R, Picano E. Radioprotection (un)awareness in cardiologists, and how to improve it. Int J Cardiovasc Imaging. 2012; 28:1369–74. [PubMed: 21850411]
12. Ditkofsky N, Shekhani HN, Cloutier M, Chen ZN, Zhang C, Hanna TN. Ionizing radiation knowledge among emergency department providers. J Am Coll Radiol. 2016; 13:1044–9.e1. [PubMed: 27162040]
13. Lam DL, Larson DB, Eisenberg JD, Forman HP, Lee CI. Communicating potential radiation-induced cancer risks from medical imaging directly to patients. AJR Am J Roentgenol. 2015; 205:962–70. [PubMed: 26295534]
14. Puri S, Hu R, Quazi RR, Voci S, Veazie P, Block R. Physicians' and midlevel providers' awareness of lifetime radiation-attributable cancer risk associated with commonly performed CT studies: relationship to practice behavior. AJR Am J Roentgenol. 2012; 199:1328–36. [PubMed: 23169726]
15. Rehani MM, Berris T. International Atomic Energy Agency study with referring physicians on patient radiation exposure and its tracking: a prospective survey using a web-based questionnaire. BMJ Open. 2012; 2:e001425.
16. Sadigh G, Khan R, Kassin MT, Applegate KE. Radiation safety knowledge and perceptions among residents: a potential improvement opportunity for graduate medical education in the United States. Acad Radiol. 2014; 21:869–78. [PubMed: 24713540]
17. Fazel R, Gerber TC, Balter S, et al. Approaches to enhancing radiation safety in cardiovascular imaging: a scientific statement from the American Heart Association. Circulation. 2014; 130:1730–48. [PubMed: 25366837]
18. International Commission on Radiological Protection. Radiological Protection in Medicine. ICRP Publication 105. Ann ICRP. 2007; 37:1–63.
19. Frush DP, Frush KS. 'Sleeping with the enemy?' Expectations and reality in imaging children in the emergency setting. Pediatr Radiol. 2008; 38(Suppl 4):S633–8. [PubMed: 18810416]
20. Gilboa SM, Devine OJ, Kucik JE, et al. Congenital heart defects in the United States: estimating the magnitude of the affected population in 2010. Circulation. 2016; 134:101–9. [PubMed: 27382105]
21. Hoffman JI, Kaplan S. The incidence of congenital heart disease. J Am Coll Cardiol. 2002; 39:1890–900. [PubMed: 12084585]
22. Lipshultz SE, Sleeper LA, Towbin JA, et al. The incidence of pediatric cardiomyopathy in two regions of the United States. N Engl J Med. 2003; 348:1647–55. [PubMed: 12711739]
23. Beausejour Ladouceur V, Lawler PR, Gurvitz M, et al. Exposure to low-dose ionizing radiation from cardiac procedures in patients with congenital heart disease: 15-year data from a population-based longitudinal cohort. Circulation. 2016; 133:12–20. [PubMed: 26538581]
24. Glatz AC, Purrington KS, Klinger A, et al. Cumulative exposure to medical radiation for children requiring surgery for congenital heart disease. J Pediatr. 2014; 164:789–94.e10. [PubMed: 24321535]
25. Johnson JN, Hornik CP, Li JS, et al. Cumulative radiation exposure and cancer risk estimation in children with heart disease. Circulation. 2014; 130:161–7. [PubMed: 24914037]

26. Cousins C, Miller DL, Bernardi G, et al. ICRP PUBLICATION 120: Radiological Protection in Cardiology. Ann ICRP. 2013; 42:1–125.
27. Taylor AJ, Cerqueira M, Hodgson JM, et al. ACCF/SCCT/ACR/AHA/ASE/ASNC/NASCI/SCAI/SCMR 2010 appropriate use criteria for cardiac computed tomography. A report of the American College of Cardiology Foundation Appropriate Use Criteria Task Force, the Society of Cardiovascular Computed Tomography, the American College of Radiology, the American Heart Association, the American Society of Echocardiography, the American Society of Nuclear Cardiology, the North American Society for Cardiovascular Imaging, the Society for Cardiovascular Angiography and Interventions, and the Society for Cardiovascular Magnetic Resonance. J Am Coll Cardiol. 2010; 56:1864–94. [PubMed: 21087721]
28. Hendel RC, Berman DS, Di Carli MF, et al. ACCF/ASNC/ACR/AHA/ASE/SCCT/SCMR/SNM 2009 appropriate use criteria for cardiac radionuclide imaging: a report of the American College of Cardiology Foundation Appropriate Use Criteria Task Force, the American Society of Nuclear Cardiology, the American College of Radiology, the American Heart Association, the American Society of Echocardiography, the Society of Cardiovascular Computed Tomography, the Society for Cardiovascular Magnetic Resonance, and the Society of Nuclear Medicine. J Am Coll Cardiol. 2009; 53:2201–29. [PubMed: 19497454]
29. Wolk MJ, Bailey SR, Doherty JU, et al. ACCF/AHA/ASE/ASNC/HFSA/HRS/SCAI/SCCT/SCMR/STS 2013 multimodality appropriate use criteria for the detection and risk assessment of stable ischemic heart disease: a report of the American College of Cardiology Foundation Appropriate Use Criteria Task Force, American Heart Association, American Society of Echocardiography, American Society of Nuclear Cardiology, Heart Failure Society of America, Heart Rhythm Society, Society for Cardiovascular Angiography and Interventions, Society of Cardiovascular Computed Tomography, Society for Cardiovascular Magnetic Resonance, and Society of Thoracic Surgeons. J Am Coll Cardiol. 2014; 63:380–406. [PubMed: 24355759]
30. Chinnaiyan KM, Peyser P, Goraya T, et al. Impact of a continuous quality improvement initiative on appropriate use of coronary computed tomography angiography. Results from a multicenter, statewide registry, the Advanced Cardiovascular Imaging Consortium. J Am Coll Cardiol. 2012; 60:1185–91. [PubMed: 22884289]
31. Lin FY, Dunning AM, Narula J, et al. Impact of an automated multimodality point-of-order decision support tool on rates of appropriate testing and clinical decision making for individuals with suspected coronary artery disease: a prospective multicenter study. J Am Coll Cardiol. 2013; 62:308–16. [PubMed: 23707319]
32. Hendel RC, Cerqueira M, Douglas PS, et al. A multicenter assessment of the use of single-photon emission computed tomography myocardial perfusion imaging with appropriateness criteria. J Am Coll Cardiol. 2010; 55:156–62. [PubMed: 20117384]
33. Doukky R, Hayes K, Frogge N, et al. Impact of appropriate use on the prognostic value of single-photon emission computed tomography myocardial perfusion imaging. Circulation. 2013; 128:1634–43. [PubMed: 24021779]
34. Saifi S, Taylor AJ, Allen J, Hendel R. The use of a learning community and online evaluation of utilization for SPECT myocardial perfusion imaging. J Am Coll Cardiol Img. 2013; 6:823–9.
35. Einstein AJ, Moser KW, Thompson RC, Cerqueira MD, Henzlova MJ. Radiation dose to patients from cardiac diagnostic imaging. Circulation. 2007; 116:1290–305. [PubMed: 17846343]
36. Report of the American Association of Physicists in Medicine Task Group 204. [Accessed January 1, 2017] Size-Specific Dose Estimates (SSDE) in Pediatric and Adult Body CT Examinations. Available at: https://www.aapm.org/pubs/reports/RPT_204.pdf
37. Deak PD, Smal Y, Kalender WA. Multisection CT protocols: sex- and age-specific conversion factors used to determine effective dose from dose-length product. Radiology. 2010; 257:158–66. [PubMed: 20851940]
38. Alessio AM, Phillips GS. A pediatric CT dose and risk estimator. Pediatr Radiol. 2010; 40:1816–21. [PubMed: 20623277]
39. Shrimpton PC, Wall BF. Reference doses for paediatric computed tomography. Radiat Prot Dosim. 2000; 90:249–52.
40. Shrimpton PC, Hillier MC, Lewis MA, Dunn M. National survey of doses from CT in the UK: 2003. Br J Radiol. 2006; 79:968–80. [PubMed: 17213302]

41. Trattner S, Chelliah A, Prinsen P, et al. Estimating effective dose of radiation from pediatric cardiac CT angiography using a 64-MDCT scanner: new conversion factors relating dose-length product to effective dose. AJR Am J Roentgenol. 2017; 208:585–94. [PubMed: 28095022]
42. Podberesky DJ, Angel E, Yoshizumi TT, et al. Radiation dose estimation for prospective and retrospective ECG-gated cardiac CT angiography in infants and small children using a 320-MDCT volume scanner. AJR Am J Roentgenol. 2012; 199:1129–35. [PubMed: 23096189]
43. Fujii K, Aoyama T, Yamauchi-Kawaura C, et al. Radiation dose evaluation in 64-slice CT examinations with adult and paediatric anthropomorphic phantoms. Br J Radiol. 2009; 82:1010–8. [PubMed: 19934069]
44. [Accessed December 16, 2016] California Senate Bill 1237. Available at: ftp://www.leginfo.ca.gov/pub/09-10/bill/sen/sb_1201-1250/sb_1237_bill_20100929_chaptered.html
45. International Commission on Radiological Protection. Radiation Dose to Patients from Radiopharmaceuticals. ICRP Publication 53. Ann ICRP. 1988; 18:1–22.
46. International Commission on Radiological Protection. Radiation Dose to Patients from Radiopharmaceuticals (Addendum to ICRP Publication 53). ICRP Publication 80. Ann ICRP. 1998; 28:1–126.
47. International Commission on Radiological Protection. Radiation Dose to Patients from Radiopharmaceuticals: Addendum 3 to ICRP Publication 53. ICRP Publication 106. Ann ICRP. 2008; 38:1–197. [PubMed: 19154964]
48. International Commission on Radiological Protection. Radiation Dose to Patients From Radiopharmaceuticals: A Compendium of Current Information Related to Frequently Used Substances. ICRP Publication 128. Ann ICRP. 2015; 44:1–319. [PubMed: 25856574]
49. Loevinger, R., Budinger, TF., Watson, EE. MIRD Primer for Absorbed Dose Calculations. Rev edition. New York, NY: Society of Nuclear Medicine; 1991.
50. Hart, D., Jones, DG., Wall, BF. Normalised Organ Doses for Paediatric X-ray Examinations Calculated Using Monte Carlo Techniques. NRPB-SR279. Chilton, UK: National Radiological Protection Board; 1996.
51. Han BK, Lesser AM, Vezmar M, et al. Cardiovascular imaging trends in congenital heart disease: a single center experience. J Cardiovasc Comput Tomogr. 2013; 7:361–6. [PubMed: 24331931]
52. Han BK, Rigsby CK, Hlavacek A, et al. Computed tomography imaging in patients with congenital heart disease part i: rationale and utility. an expert consensus document of the Society of Cardiovascular Computed Tomography (SCCT). J Cardiovasc Comput Tomogr. 2015; 9:475–92. [PubMed: 26272851]
53. Hlavacek AM. Imaging of congenital cardiovascular disease: the case for computed tomography. J Thorac Imaging. 2010; 25:247–55. [PubMed: 20711041]
54. Ben Saad M, Rohnean A, Sigal-Cinqualbre A, Adler G, Paul JF. Evaluation of image quality and radiation dose of thoracic and coronary dualsource CT in 110 infants with congenital heart disease. Pediatr Radiol. 2009; 39:668–76. [PubMed: 19319514]
55. Paul JF, Rohnean A, Elfassy E, Sigal-Cinqualbre A. Radiation dose for thoracic and coronary step-and-shoot CT using a 128-slice dual-source machine in infants and small children with congenital heart disease. Pediatr Radiol. 2011; 41:244–9. [PubMed: 20821005]
56. Watson TG, Mah E, Joseph Schoepf U, King L, Huda W, Hlavacek AM. Effective radiation dose in computed tomographic angiography of the chest and diagnostic cardiac catheterization in pediatric patients. Pediatr Cardiol. 2013; 34:518–24. [PubMed: 22956060]
57. Srivastava S, Printz BF, Geva T, et al. Task Force 2: Pediatric Cardiology Fellowship Training in Noninvasive Cardiac Imaging. J Am Coll Cardiol. 2015; 66:687–98. [PubMed: 25777631]
58. Han BK, Rigsby CK, Leipsic J, et al. Computed tomography imaging in patients with congenital heart disease, part 2: technical recommendations. An expert consensus document of the Society of Cardiovascular Computed Tomography (SCCT). J Cardiovasc Comput Tomogr. 2015; 9:493–513. [PubMed: 26679548]
59. Goske MJ, Applegate KE, Boylan J, et al. The 'Image Gently' campaign: increasing CT radiation dose awareness through a national education and awareness program. Pediatr Radiol. 2008; 38:265–9. [PubMed: 18202842]

60. Gherardi GG, Iball GR, Darby MJ, Thomson JD. Cardiac computed tomography and conventional angiography in the diagnosis of congenital cardiac disease in children: recent trends and radiation doses. Cardiol Young. 2011; 21:616–22. [PubMed: 21733206]

61. de Graaf FR, Schuijf JD, van Velzen JE, et al. Evaluation of contraindications and efficacy of oral Beta blockade before computed tomographic coronary angiography. Am J Cardiol. 2010; 105:767–72. [PubMed: 20211317]

62. Achenbach S, Manolopoulos M, Schuhback A, et al. Influence of heart rate and phase of the cardiac cycle on the occurrence of motion artifact in dual-source CT angiography of the coronary arteries. J Cardiovasc Comput Tomogr. 2012; 6:91–8. [PubMed: 22381662]

63. Chelliah A, Kubacki T, Julien HM, Einstein AJ. Pediatric coronary CTA using phenylephrine to lower heart rate. J Cardiovasc Comput Tomogr. 2016; 10:339–40. [PubMed: 27363865]

64. Weustink AC, Neefjes LA, Kyrzopoulos S, et al. Impact of heart rate frequency and variability on radiation exposure, image quality, and diagnostic performance in dual-source spiral CT coronary angiography. Radiology. 2009; 253:672–80. [PubMed: 19864512]

65. Karlo C, Leschka S, Goetti RP, et al. High-pitch dual-source CT angiography of the aortic valve-aortic root complex without ECG-synchronization. Eur Radiol. 2011; 21:205–12. [PubMed: 20677006]

66. Lell MM, May M, Deak P, et al. High-pitch spiral computed tomography: effect on image quality and radiation dose in pediatric chest computed tomography. Invest Radiol. 2011; 46:116–23. [PubMed: 20856124]

67. Schernthaner RE, Stadler A, Beitzke D, et al. Dose modulated retrospective ECG-gated versus non-gated 64-row CT angiography of the aorta at the same radiation dose: comparison of motion artifacts, diagnostic confidence and signal-to-noise-ratios. Eur J Radiol. 2012; 81:e585–90. [PubMed: 21820829]

68. Shuman WP, Leipsic JA, Busey JM, et al. Prospectively ECG gated CT pulmonary angiography versus helical ungated CT pulmonary angiography: impact on cardiac related motion artifacts and patient radiation dose. Eur J Radiol. 2012; 81:2444–9. [PubMed: 21703791]

69. Lesser JR, Flygenring BJ, Knickelbine T, Longe T, Schwartz RS. Practical approaches to overcoming artifacts in coronary CT angiography. J Cardiovasc Comput Tomogr. 2009; 3:4–15. [PubMed: 19201371]

70. Li J, Udayasankar UK, Toth TL, Seamans J, Small WC, Kalra MK. Automatic patient centering for MDCT: effect on radiation dose. AJR Am J Roentgenol. 2007; 188:547–52. [PubMed: 17242267]

71. Siegel MJ, Ramirez-Giraldo JC, Hildebolt C, Bradley D, Schmidt B. Automated low-kilovoltage selection in pediatric computed tomography angiography: phantom study evaluating effects on radiation dose and image quality. Invest Radiol. 2013; 48:584–9. [PubMed: 23563195]

72. Zhang LJ, Qi L, Wang J, et al. Feasibility of prospectively ECG-triggered high-pitch coronary CT angiography with 30 mL iodinated contrast agent at 70 kVp: initial experience. Eur Radiol. 2014; 24:1537–46. [PubMed: 24737530]

73. Pache G, Grohmann J, Bulla S, et al. Prospective electrocardiography-triggered CT angiography of the great thoracic vessels in infants and toddlers with congenital heart disease: feasibility and image quality. Eur J Radiol. 2011; 80:e440–5. [PubMed: 21310567]

74. Stolzmann P, Goetti R, Baumueller S, et al. Prospective and retrospective ECG-gating for CT coronary angiography perform similarly accurate at low heart rates. Eur J Radiol. 2011; 79:85–91. [PubMed: 20079993]

75. Mahnken AH, Bruners P, Schmidt B, Bornikoel C, Flohr T, Gunther RW. Left ventricular function can reliably be assessed from dual-source CT using ECG-gated tube current modulation. Invest Radiol. 2009; 44:384–9. [PubMed: 19448556]

76. Leipsic J, LaBounty TM, Ajlan AM, et al. A prospective randomized trial comparing image quality, study interpretability, and radiation dose of narrow acquisition window with widened acquisition window protocols in prospectively ECG-triggered coronary computed tomography angiography. J Cardiovasc Comput Tomogr. 2013; 7:18–24. [PubMed: 23452996]

77. Goetti R, Feuchtner G, Stolzmann P, et al. High-pitch dual-source CT coronary angiography: systolic data acquisition at high heart rates. Eur Radiol. 2010; 20:2565–71. [PubMed: 20585785]

78. Herzog C, Mulvihill DM, Nguyen SA, et al. Pediatric cardiovascular CT angiography: radiation dose reduction using automatic anatomic tube current modulation. AJR Am J Roentgenol. 2008; 190:1232–40. [PubMed: 18430837]

79. Ghoshhajra BB, Lee AM, Engel LC, et al. Radiation dose reduction in pediatric cardiac computed tomography: experience from a tertiary medical center. Pediatr Cardiol. 2014; 35:171–9. [PubMed: 23872908]

80. Ghoshhajra BB, Engel LC, Karolyi M, et al. Cardiac computed tomography angiography with automatic tube potential selection: effects on radiation dose and image quality. J Thorac Imaging. 2013; 28:40–8. [PubMed: 22847638]

81. Han BK, Grant KL, Garberich R, Sedlmair M, Lindberg J, Lesser JR. Assessment of an iterative reconstruction algorithm (SAFIRE) on image quality in pediatric cardiac CT datasets. J Cardiovasc Comput Tomogr. 2012; 6:200–4. [PubMed: 22682262]

82. Mieville FA, Gudinchet F, Rizzo E, et al. Paediatric cardiac CT examinations: impact of the iterative reconstruction method ASIR on image quality–preliminary findings. Pediatr Radiol. 2011; 41:1154–64. [PubMed: 21717165]

83. Mattsson S, Johansson L, Leide Svegborn S, et al. Radiation dose to patients from radiopharmaceuticals: a compendium of current information related to frequently used substances. Ann ICRP. 2015; 44:7–321.

84. Mercuri M, Pascual TN, Mahmarian JJ, et al. Estimating the reduction in the radiation burden from nuclear cardiology through use of stress-only imaging in the United States and Worldwide. JAMA Intern Med. 2016; 176:269–73. [PubMed: 26720615]

85. Guner LA, Caliskan B, Isik I, Aksoy T, Vardareli E, Parspur A. Evaluating the role of routine prone acquisition on visual evaluation of SPECT images. J Nucl Med Technol. 2015; 43:282–8. [PubMed: 26584617]

86. Einstein AJ, Pascual TN, Mercuri M, et al. Current worldwide nuclear cardiology practices and radiation exposure: results from the 65 country IAEA Nuclear Cardiology Protocols Cross-Sectional Study (INCAPS). Eur Heart J. 2015; 36:1689–96. [PubMed: 25898845]

87. Treves ST, Gelfand MJ, Fahey FH, Parisi MT. 2016 update of the North American Consensus Guidelines for Pediatric Administered Radiopharmaceutical Activities. J Nucl Med. 2016; 57:15N–8N. [PubMed: 26514173]

88. [Accessed December 1, 2016] EANM Dosage Card (Version 5.7.2016). Available at: http://www.eanm.org/docs/EANM_Dosage_Card_040214.pdf

89. Ait-Ali L, Andreassi MG, Foffa I, Spadoni I, Vano E, Picano E. Cumulative patient effective dose and acute radiation-induced chromosomal DNA damage in children with congenital heart disease. Heart. 2010; 96:269–74. [PubMed: 19687017]

90. Walsh MA, Noga M, Rutledge J. Cumulative radiation exposure in pediatric patients with congenital heart disease. Pediatr Cardiol. 2015; 36:289–94. [PubMed: 25124721]

91. Brown PH, Thomas RD, Silberberg PJ, Johnson LM. Optimization of a fluoroscope to reduce radiation exposure in pediatric imaging. Pediatr Radiol. 2000; 30:229–35. [PubMed: 10789900]

92. Hill KD, Wang C, Einstein AJ, et al. Impact of imaging approach on radiation dose and associated cancer risk in children undergoing cardiac catheterization. Catheter Cardiovasc Interv. 2017; 89:888–97. [PubMed: 27315598]

93. Stueve D. Management of pediatric radiation dose using Philips fluoroscopy systems DoseWise: perfect image, perfect sense. Pediatr Radiol. 2006; 36(Suppl 2):216–20.

94. Strauss KJ. Pediatric interventional radiography equipment: safety considerations. Pediatr Radiol. 2006; 36(Suppl 2):126–35.

95. Strauss KJ. Interventional suite and equipment management: cradle to grave. Pediatr Radiol. 2006; 36(Suppl 2):221–36. [PubMed: 16862407]

96. Justino H. The ALARA concept in pediatric cardiac catheterization: techniques and tactics for managing radiation dose. Pediatr Radiol. 2006; 36(Suppl 2):146–53. [PubMed: 16862415]

97. Ubeda C, Vano E, Gonzalez L, Miranda P. Influence of the antiscatter grid on dose and image quality in pediatric interventional cardiology X-ray systems. Catheter Cardiovasc Interv. 2013; 82:51–7. [PubMed: 22899572]

98. Partridge J, McGahan G, Causton S, et al. Radiation dose reduction without compromise of image quality in cardiac angiography and intervention with the use of a flat panel detector without an antiscatter grid. Heart. 2006; 92:507–10. [PubMed: 16159965]

99. Drago F, Silvetti MS, Di Pino A, Grutter G, Bevilacqua M, Leibovich S. Exclusion of fluoroscopy during ablation treatment of right accessory pathway in children. J Cardiovasc Electrophysiol. 2002; 13:778–82. [PubMed: 12212697]

100. Mah DY, Miyake CY, Sherwin ED, et al. The use of an integrated electroanatomic mapping system and intracardiac echocardiography to reduce radiation exposure in children and young adults undergoing ablation of supraventricular tachycardia. Europace. 2014; 16:277–83. [PubMed: 23928735]

101. Miyake CY, Mah DY, Atallah J, et al. Nonfluoroscopic imaging systems reduce radiation exposure in children undergoing ablation of supraventricular tachycardia. Heart Rhythm. 2011; 8:519–25. [PubMed: 21167315]

102. Papagiannis J, Avramidis D, Alexopoulos C, Kirvassilis G. Radiofrequency ablation of accessory pathways in children and congenital heart disease patients: impact of a nonfluoroscopic navigation system. Pacing Clin Electrophysiol. 2011; 34:1288–396. [PubMed: 21851369]

103. Smith G, Clark JM. Elimination of fluoroscopy use in a pediatric electrophysiology laboratory utilizing three-dimensional mapping. Pacing Clin Electrophysiol. 2007; 30:510–8. [PubMed: 17437575]

104. Tuzcu V. Significant reduction of fluoroscopy in pediatric catheter ablation procedures: long-term experience from a single center. Pacing Clin Electrophysiol. 2012; 35:1067–73. [PubMed: 22817263]

105. Gellis LA, Ceresnak SR, Gates GJ, Nappo L, Pass RH. Reducing patient radiation dosage during pediatric SVT ablations using an “ALARA” radiation reduction protocol in the modern fluoroscopic era. Pacing Clin Electrophysiol. 2013; 36:688–94. [PubMed: 23510152]

106. Verghese GR, McElhinney DB, Strauss KJ, Bergersen L. Characterization of radiation exposure and effect of a radiation monitoring policy in a large volume pediatric cardiac catheterization lab. Catheter Cardiovasc Interv. 2012; 79:294–301. [PubMed: 21523897]

107. Raff GL, Chinnaiyan KM, Share DA, et al. Radiation dose from cardiac computed tomography before and after implementation of radiation dose-reduction techniques. JAMA. 2009; 301:2340–8. [PubMed: 19509381]

108. Society for Cardiovascular Angiography and Interventions. [Accessed April 1, 2017] Pediatric SCAI-QIT: Pediatric Radiation Safety Quality Improvement Toolkit. Available at: http://www.scai.org/pedqit/default.aspx

109. Hartwig HD, Clingenpeel J, Perkins AM, Rose W, Abdullah-Anyiwo J. Parental knowledge of radiation exposure in medical imaging used in the pediatric emergency department. Pediatr Emerg Care. 2013; 29:705–9. [PubMed: 23714757]

110. Larson DB, Rader SB, Forman HP, Fenton LZ. Informing parents about CT radiation exposure in children: it’s OK to tell them. AJR Am J Roentgenol. 2007; 189:271–5. [PubMed: 17646450]

111. Frush DP. The role of CT in professionalism: accreditation, certification and the welfare of our children. Pediatr Radiol. 2011; 41(Suppl 2):571–5. [PubMed: 21847741]

112. Sox HC. Disease prevention guidelines from the U.S. Preventive Services Task Force. Ann Intern Med. 2002; 136:155–6. [PubMed: 11790070]

113. Westra SJ. The communication of the radiation risk from CT in relation to its clinical benefit in the era of personalized medicine: part 2: benefits versus risk of CT. Pediatr Radiol. 2014; 44(Suppl 3):525–33. [PubMed: 25304716]

114. Pinyavat T, Warner DO, Flick RP, et al. Summary of the Update Session on Clinical Neurotoxicity Studies. J Neurosurg Anesthesiol. 2016; 28:356–60. [PubMed: 27768673]

115. Blumfield E, Moore MM, Drake MK, et al. Survey of gadolinium-based contrast agent utilization among the members of the Society for Pediatric Radiology: a Quality and Safety Committee report. Pediatr Radiol. 2017; 47:665–73. [PubMed: 28283728]

116. Callahan MJ, Poznauskis L, Zurakowski D, Taylor GA. Nonionic iodinated intravenous contrast material-related reactions: incidence in large urban children’s hospital—retrospective analysis of data in 12,494 patients. Radiology. 2009; 250:674–81. [PubMed: 19244041]

117. Einstein AJ, Berman DS, Min JK, et al. Patient-centered imaging: shared decision making for cardiac imaging procedures with exposure to ionizing radiation. J Am Coll Cardiol. 2014; 63:1480–9. [PubMed: 24530677]

118. Perez, M., Miller, D., Frush, DP., et al. World Health Organization. [Accessed December 13, 2016] Communicating Radiation Risks in Pediatric Imaging to Support Risk-Benefit Dialogue: Information to Support Healthcare Discussions About Benefit and Risk. 2016. Available at: http://www.who.int/ionizing_radiation/pub_meet/radiationrisks-paediatric-imaging/en/

119. Nievelstein RA, Frush DP. Should we obtain informed consent for examinations that expose patients to radiation? AJR Am J Roentgenol. 2012; 199:664–9. [PubMed: 22915409]

120. Frush D, Denham CR, Goske MJ, et al. Radiation protection and dose monitoring in medical imaging: a journey from awareness, through accountability, ability and action...but where will we arrive? J Patient Saf. 2013; 9:232–8. [PubMed: 24257067]

121. The Joint Commission. [Accessed December 13, 2016] Diagnostic Imaging Requirements. Aug 10. 2015 Available at: http://www.jointcommission.org/assets/1/18/AHC_DiagImagingRpt_MK_20150806.pdf

122. American College of Radiology. [Accessed December 13, 2016] Dose Index Registry. Available at: https://www.acr.org/Quality-Safety/National-Radiology-Data-Registry/Dose-Index-Registry

123. American Society of Nuclear Cardiology. [Accessed December 13, 2016] ImageGuide Registry: Cardiovascular Imaging Data Registry. American Society of Nuclear Cardiology. Available at: http://www.asnc.org/imageguide

124. Young LH, Wackers FJ, Chyun DA, et al. Cardiac outcomes after screening for asymptomatic coronary artery disease in patients with type 2 diabetes: the DIAD study: a randomized controlled trial. JAMA. 2009; 301:1547–55. [PubMed: 19366774]

125. Douglas PS, Hoffmann U, Patel MR, et al. Outcomes of anatomical versus functional testing for coronary artery disease. N Engl J Med. 2015; 372:1291–300. [PubMed: 25773919]

126. SCOT-HEART Investigators. CT coronary angiography in patients with suspected angina due to coronary heart disease (SCOT-HEART): an open-label, parallel-group, multicentre trial. Lancet. 2015; 385:2383–91. [PubMed: 25788230]

127. Beanlands RS, Nichol G, Huszti E, et al. F-18-fluorodeoxyglucose positron emission tomography imaging-assisted management of patients with severe left ventricular dysfunction and suspected coronary disease: a randomized, controlled trial (PARR-2). J Am Coll Cardiol. 2007; 50:2002–12. [PubMed: 17996568]

128. Cousins C. ICRP and radiological protection in medicine. Radiat Prot Dosimetry. 2017; 173:177–9. [PubMed: 27895096]

129. International Electrotechnical Commission. [Accessed December 16, 2016] IEC 61267:2005 Medical Diagnostic X-Ray Equipment-Radiation Conditions for Use in the Determination of Characteristics. 22005. Available at: http://www.iec.ch/dyn/www/f?p=103:22:0::::FSP_ORG_ID:1362

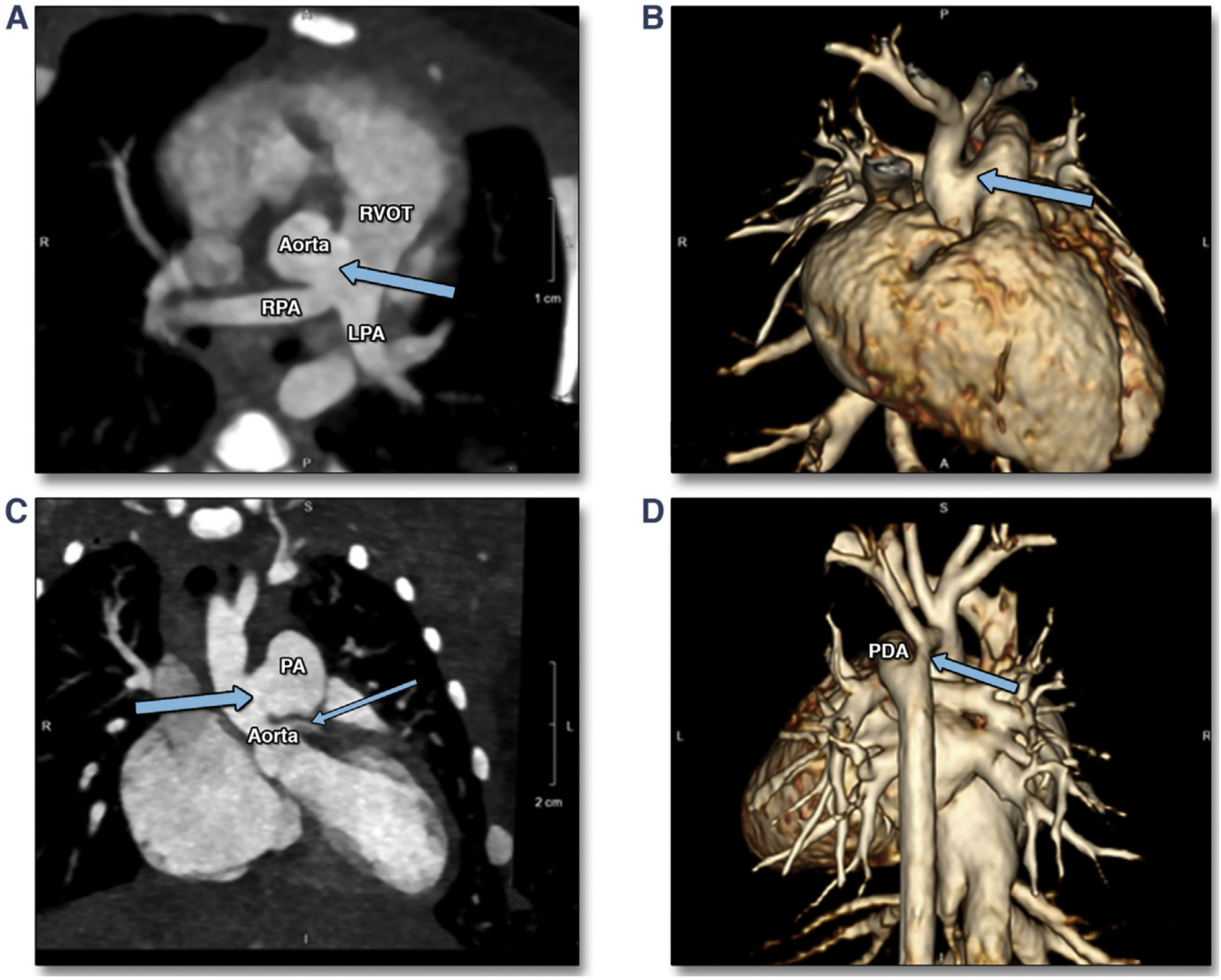

FIGURE 1. Case Illustrating Low-Dose Cardiac CT in Children

This CT scan was performed in a 1-day-old patient (2.8 kg) with an aortopulmonary (AP) window and aortic coarctation to further define great arterial anatomy. The patient was free breathing and without sedation (heart rate 145 beats/min). A total of 5.5 ml of iodinated contrast was mixed with an equivalent volume of saline and delivered via power injector through a 22-ga peripheral intravenous line placed in the left antecubital vein at a rate of 1 ml/s. The scan was performed on a third-generation dual source CT scanner (Somatom Force, Siemens Medical, Forchheim, Germany). Scan specifications included: 2 × 96 detector rows, 0.25-s gantry rotation time, 66-ms temporal resolution, 730-mm/s table acquisition speed. A prospectively ECG-triggered high-pitch (3.2) helical scan mode was used with 70-kVp tube voltage, automatic exposure control with online modulation (CARE Dose4D, Siemens Medical). The CT dose–volume index (CTDIvol) was 0.23 mGy, and the scan dose–length product (DLP) was 2.9 mGy · cm. Data were processed using a model-based iterative reconstruction algorithm with a strength of 3. An isovolumetric 0.5-mm dataset was analyzed on a dedicated 3D workstation (Vitrea Enterprise Viewer, Vital Images,

Minnetonka, Minnesota). **A** shows a 2D image showing the AP window **(arrow)** relationship to the branch pulmonary arteries, with the distal end of the defect extending to the proximal right pulmonary artery (RPA). **B** shows a 3D reconstruction showing the AP window **(arrow)** between the ascending aorta and proximal main pulmonary artery (PA). **C** illustrates the origin of the left main coronary artery **(thin arrow)** from the superior aspect of the sinus of Valsalva, 1.5 mm from the inferior margin of the AP window **(thick arrow).** **D** shows a 3D posterior view of the aortic coarctation **(arrow)** and a large patent ductus arteriosus (PDA). Images courtesy of B. Kelly Han, MD, and John R Lesser, MD. Children's Heart Clinic at the Children's Hospitals and Clinics of Minnesota and the Minneapolis Heart Institute. Minneapolis, Minnesota. 2D = 2-dimensional; 3D = 3-dimensional; CT = computed tomography; ECG = electrocardiogram; LPA = left pulmonary artery; RVOT = right ventricular outflow tract.

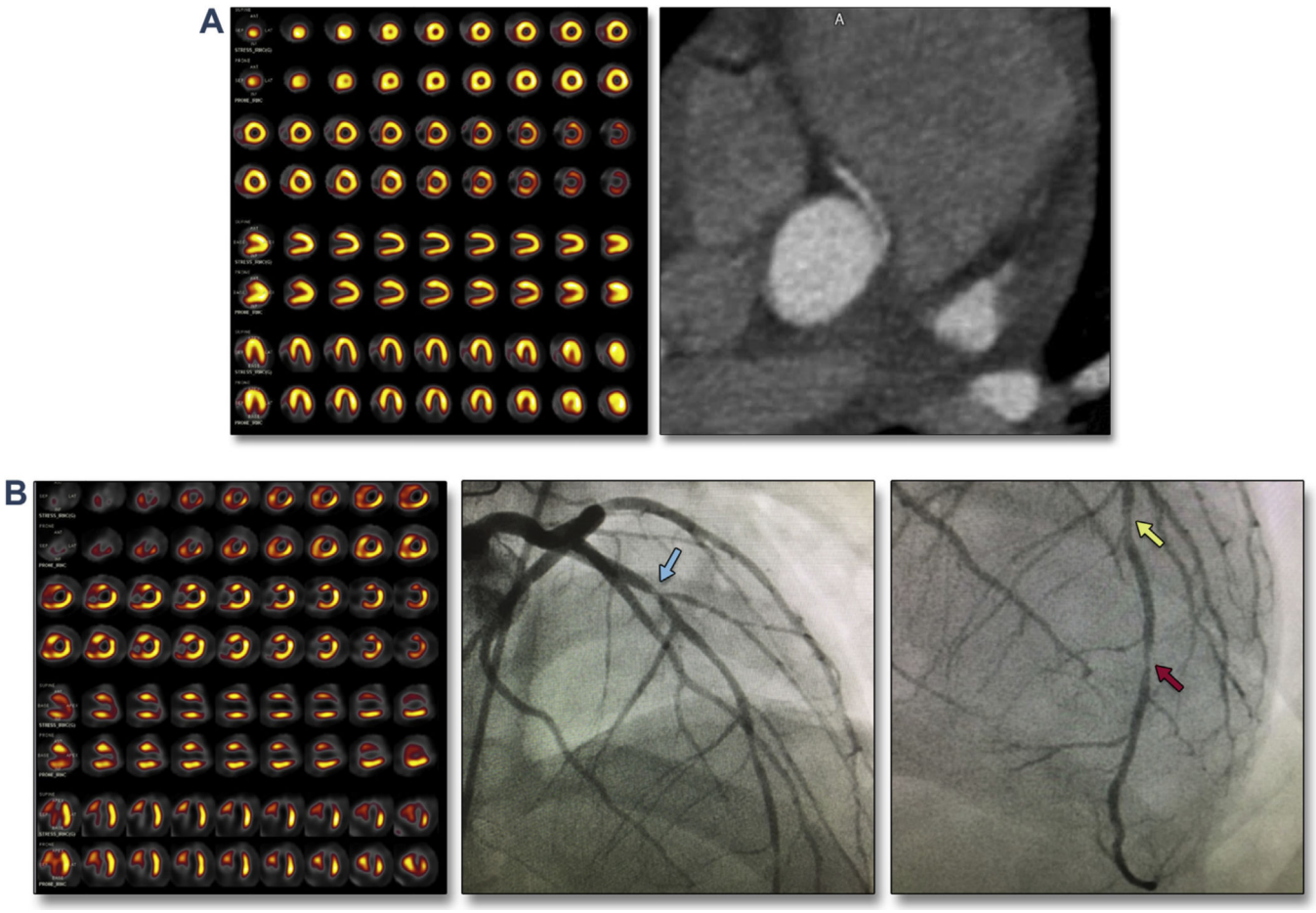

FIGURE 2. Cases Illustrating Low-Dose Stress Myocardial Perfusion Imaging in Children

(A) Normal post-operative supine **(upper rows, left)** and prone **(lower rows, left)** stress-only imaging performed on a high-efficiency single-photon emission computed tomography (SPECT) camera with 5.2 mCi of Tc-99m sestamibi, in a 5'6", 158-lb 15-year-old boy. The patient had had recurrent episodes of exertional chest pain, and a coronary CT angiogram (**right**; 2 mm maximal intensity projection, 100 kV, 200 mA, dose-length product 29 mGy · cm) revealed an anomalous right coronary artery off of the left cusp, with a small, slit-like ostium, acute takeoff, and intramural intervascular course. He underwent unroofing surgery 4 months before the nuclear stress test. **(B)** Stress-only imaging performed on a high-efficiency SPECT camera with 3.5 mCi of Tc-99m sestamibi, in a 5'2", 103-lb 14-year-old boy 6 years postorthotopic heart transplant with transplant coronary artery disease and prior drug-eluting stent of the distal left circumflex artery. Exercise electrocardiography revealed up to 1 mm of ST-segment elevations in leads V_1 to V_3 and up to 1 mm of horizontal ST-segment depressions in leads III, aVF, V_5, and V_6, which persisted 6 min into recovery. Stress supine **(upper rows, left)** and prone **(lower rows, left)** perfusion imaging above revealed anterior, anterolateral, apical, and basal septal perfusion defects that had not been observed on rest imaging on a nuclear stress test the prior year. After discussion with the referring physician, rest imaging was omitted and the patient referred for coronary angiography **(middle and right)**, which revealed stenoses in the proximal (75%; **blue**

arrow), mid (70%; **yellow arrow**), and distal (90%; **red arrow**) left anterior descending artery, and a patent stent in the circumflex. He received a drug-eluting stent in the proximal vessel, and balloon angioplasty of the mid and distal segments. Images courtesy of Michael Collins MD, Ketan Bhattia CNMT, and Andrew J. Einstein MD, PhD, Columbia University Medical Center/New York-Presbyterian Hospital.

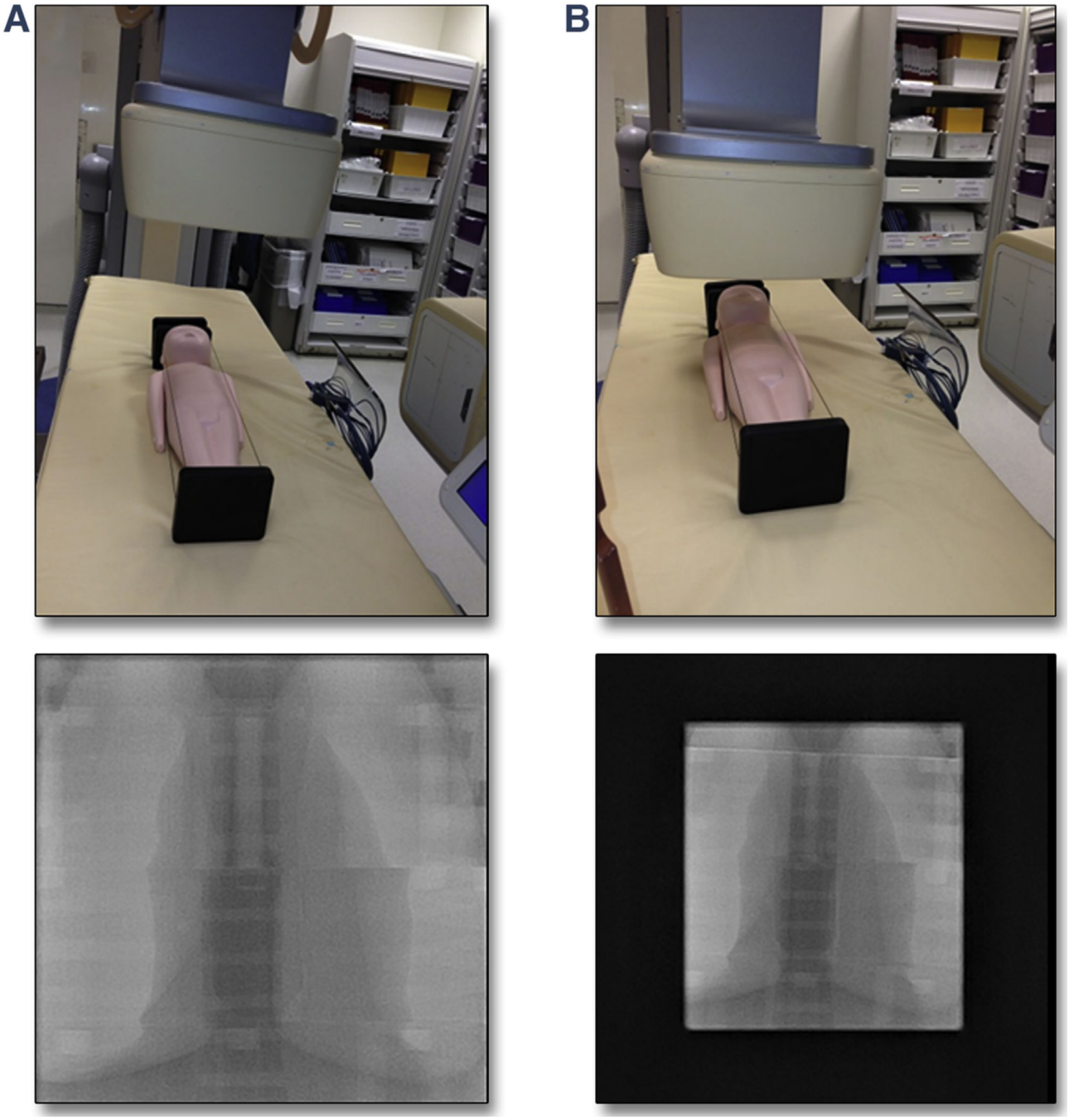

FIGURE 3. Effects of Operator-Dependent Approaches to Dose Management

In **A**, the image receptor is raised 20 cm from the patient (source-to-image distance [SID] = 113 cm), electronic magnification is increased (6-inch field of view [FOV]), and there is no collimation. In **B**, the image receptor is lowered to the patient (93 cm SID), electronic magnification is reduced 1 step (8-inch FOV), and the image is maximally collimated on all sides. The effective dose to the phantom (approximating a 3.5-kg, 51-cm neonate) for fluoroscopy in **A** was 0.74 mSv/min versus 0.27 mSv/min in **B**, a 2.7-fold reduction. Depending on the type of diagnostic or interventional procedure being performed, this

reduced level of magnification may be adequate, and can achieve significant radiation reduction. With removal of the anti-scatter grid, the dose is further reduced to 0.14 mSv/min.

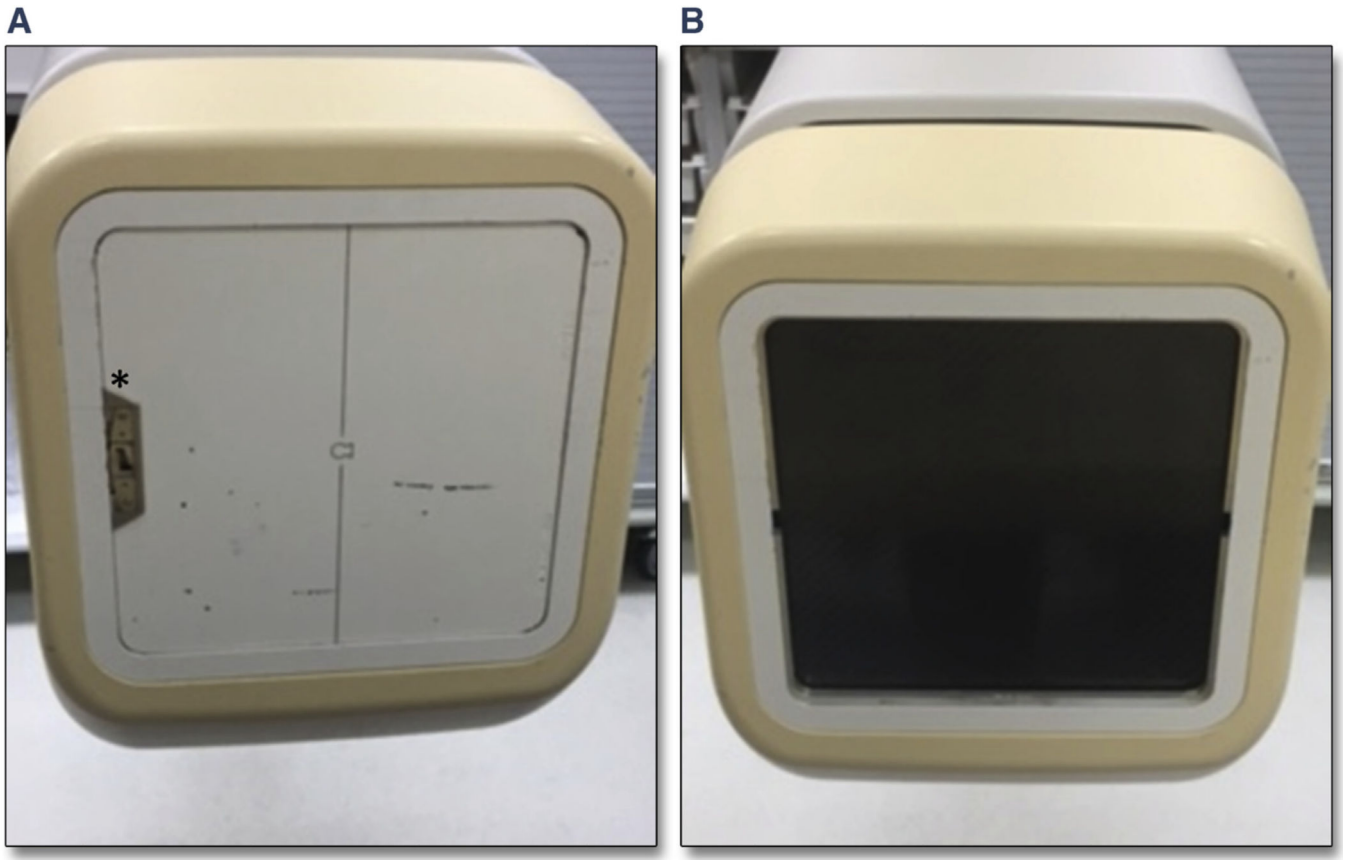

FIGURE 4. Anti-Scatter Grid Removal

The receptor from a Philips Allura XPER (Philips, Amsterdam, the Netherlands) system is demonstrated with the anti-scatter grid in place **(A)** and removed **(B)**. On this particular system, the grid can be removed easily using the locking mechanism seen in **A (asterisk)**.

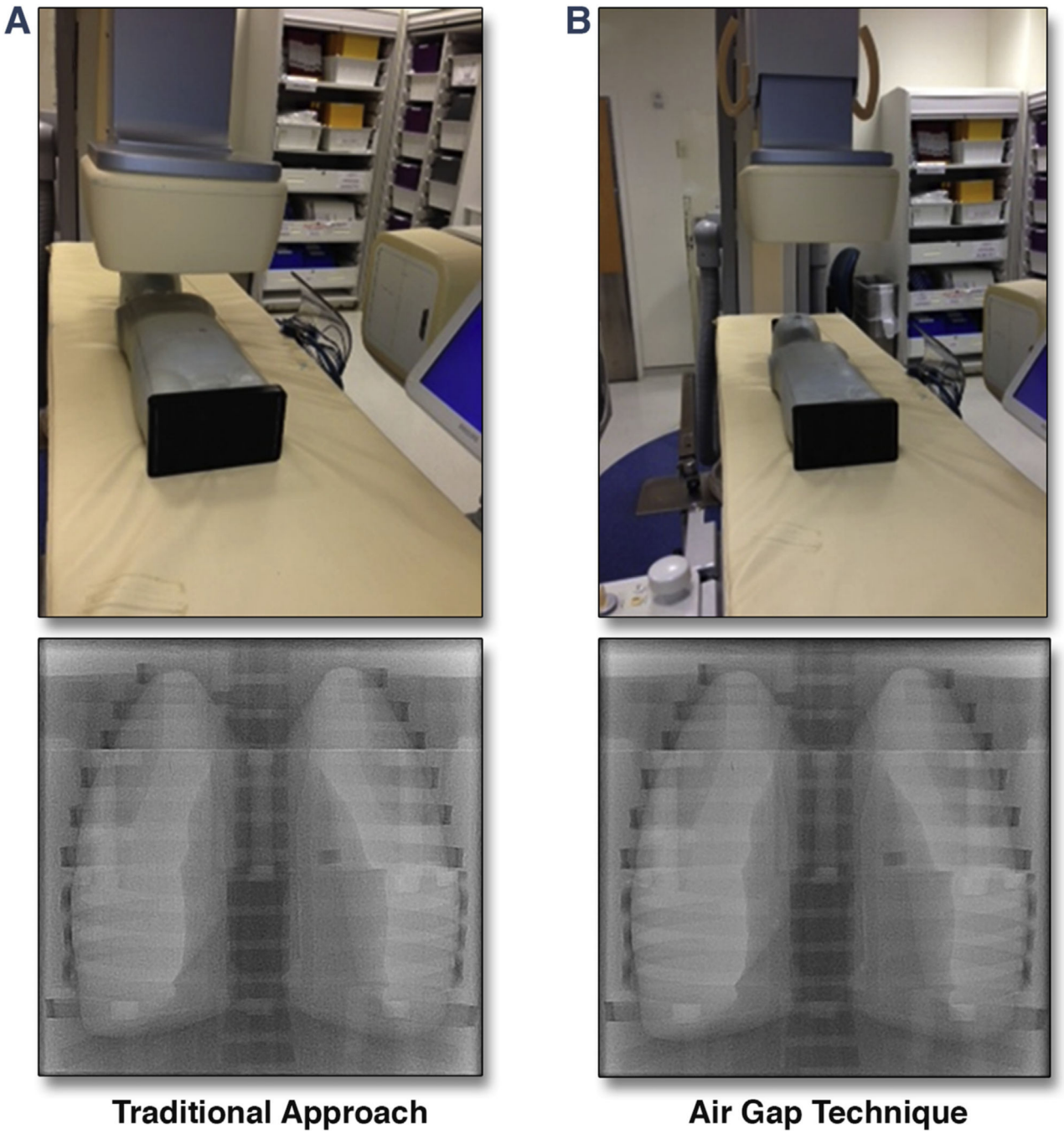

FIGURE 5. Air Gap Technique

(A) Phantom imaging using a phantom representing a 3.5-kg, 51-cm neonate, is performed with a traditional setup including SID of 91 cm (image receptor 15 cm from phantom, lowest achievable), 8-inch FOV and the anti-scatter grid in place. **(B)** Phantom imaging using the air gap approach. The anti-scatter grid has been removed, the receptor is raised 15 cm (SID = 106 cm), and the FOV has been increased to 10-inch (1-step reduction in electronic magnification). Both images are collimated on the periphery. On this particular fluoroscope,

the air gap technique achieves a similar appearing image, but dose-area product for this 20-s acquisition is reduced from 3.76 mSv in **A** to 2.79 mSv in **B**. Abbreviations as in Figure 4.

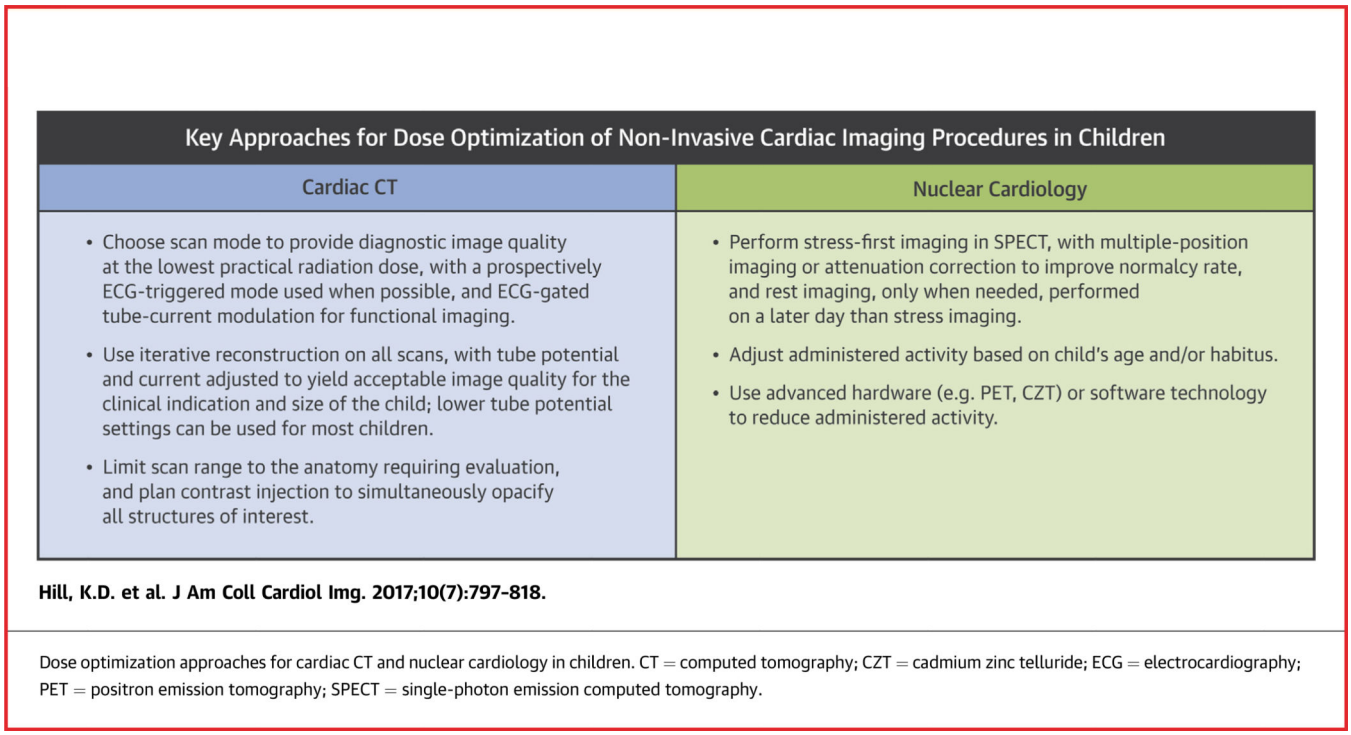

CENTRAL ILLUSTRATION. Key Approaches for Dose Optimization of Non-Invasive Cardiac Imaging Procedures in Children

JACC Cardiovasc Imaging. Author manuscript; available in PMC 2018 July 01.

TABLE 1

Pediatric Cardiac and Chest CT Conversion Factors Relating DLP to ED in Children

Age (Yrs)	Scan Region	Conversion Factor (mean) ($mSv \cdot mGy^{-1} \cdot cm^{-1}$) Normalized to 32-cm Phantom*	ICRP Publication for ED Definition	Scanner Model (Manufacturer)	No. of Scanner Slices	Scan Length (cm)	Conversion Factor (Mean) ($mSv \cdot mGy^{-1} \cdot cm^{-1}$) Non-normalized	CTDI Phantom Size (cm)	First Author (Ref. #)
Newborn	Chest	0.0739	103	Siemens Somatom Sensation	64	7.56	0.0739	32	Deak et al. (37)
	Chest	0.114	103	GE LightSpeed VCT	64	9	0.057	16	Alessio and Phillips (38)
	Chest	0.0684	60	Siemens Somatom Sensation	64	7.56	0.0684	32	Deak et al. (37)
	Chest	0.078	60	First-generation Siemens Somatom DRH, GE OEC 9800, and Philips LX 3	1	9	0.039	16	Shrimpton et al. (39,40)
1	**Cardiac**	**0.099**	**103**	**GE LightSpeed VCT XTe**	**64**	**6.9**	**0.099**	**32**	**Trattner et al. (41)**
	Cardiac	**0.092†**	**103**	**Toshiba Aquilion ONE**	**320**	**10**	**0.046**	**16**	**Podberesky et al. (42)**
	Chest	0.0482	103	Siemens Somatom Sensation	64	10.75	0.0482	32	Deak et al. (37)
	Chest	0.076	103	GE LightSpeed VCT	64	12	0.038	16	Alessio and Phillips (38)
	Cardiac	0.076	60	GE LightSpeed VCT XTe	64	6.9	0.076	32	Trattner et al. (41)
	Chest	0.0443	60	Siemens Somatom Sensation	64	10.75	0.0443	32	Deak et al. (37)
	Chest	0.052	60	First-generation Siemens Somatom DRH, GE OEC 9800, and Philips LX 3	1	12	0.026	16	Shrimpton et al. (39,40)
5	**Cardiac**	**0.085‡**	**103**	**Toshiba Aquilion ONE**	**320**	**10**	**0.085‡**	**32**	**Podberesky et al. (42)**
	Cardiac	**0.090§**	**103**	**Toshiba Aquilion ONE**	**320**	**10**	**0.090§**	**32**	**Podberesky et al. (42)**
	Chest	0.0323	103	Siemens Somatom Sensation	64	14.17	0.0323	32	Deak et al. (37)
	Chest	0.052	103	GE LightSpeed VCT	64	16	0.026	16	Alessio and Phillips (38)
	Chest	0.0299	60	Siemens Somatom Sensation	64	14.17	0.0299	32	Deak et al. (37)
	Chest	0.036	60	First-generation Siemens Somatom DRH, GE OEC 9800, and Philips LX 3	1	16	0.018	16	Shrimpton et al. (39,40)
6	Chest	0.048	103	Toshiba, GE, Siemens, Philips (models not named)	64	21.8–30.0	0.048	32	Fujii et al. (43)
10	**Cardiac**	**0.049**	**103**	**GE LightSpeed VCT XTe**	**64**	**10.55**	**0.049**	**32**	**Trattner et al. (41)**
	Chest	0.0237	103	Siemens Somatom Sensation	64	17.75	0.0237	32	Deak et al. (37)
	Chest	0.038	103	GE LightSpeed VCT	64	20	0.019	16	Alessio and Phillips (38)

Age (Yrs)	Scan Region	Conversion Factor (mean) ($mSv \cdot mGy^{-1} \cdot cm^{-1}$) Normalized to 32-cm Phantom*	ICRP Publication for ED Definition	Scanner Model (Manufacturer)	No. of Scanner Slices	Scan Length (cm)	Conversion Factor (Mean) ($mSv \cdot mGy^{-1} \cdot cm^{-1}$) Non-normalized	CTDI Phantom Size (cm)	First Author (Ref. #)
	Cardiac	0.034	60	GE LightSpeed VCT XTe	64	10.55	0.034	32	Trattner et al. (41)
	Chest	0.0221	60	Siemens Somatom Sensation	64	17.75	0.0221	32	Deak et al. (37)
	Chest	0.026	60	First-generation Siemens Somatom DRH, GE OEC 9800, and Philips LX 3	1	20	0.013	16	Shrimpton et al. (39,40)

ED is estimated by multiplying DLP by conversion factor. **Bold type** highlights cardiac-specific conversion factors determined using ICRP Publication 103 (2) definition of ED, which reflects optimal protocol and definition for estimation of ED for a cardiac CT scan. Average cardiothoracic conversion factors using ICRP 103 definition of ED are provided in Table 2.

*For experiments performed with 16-cm phantom, the conversion factor here is normalized to 32-cm phantom by a factor of 2.0.

†Using a factor of 1.9 which was determined on the CT scanner for this specific work, instead of a factor of 2.0, which would yield a normalized conversion factor of 0.087.

‡For 60 beats/min.

§For 120 beats/min.

CT = computed tomography; CTDI = computed tomography dose index; DLP = dose–length product; ED = effective dose.

TABLE 2

Pediatric Average Cardiothoracic CT Conversion Factors Relating DLP to ED in Children

Category	Average Conversion Factor for 32-cm Phantom ($mSv \cdot mGy^{-1} \cdot cm^{-1}$)	Average Conversion Factor for 16-cm Phantom ($mSv \cdot mGy^{-1} \cdot cm^{-1}$)
Newborn	0.085	0.043
1-year-old	0.079	0.039
5-year-old	0.065	0.032
10-year-old	0.037	0.018

Determined based on average of cardiothoracic conversion factors in Table 1 that were calculated using ICRP 103 tissue weighting factors (approved by the American Association of Physicists in Medicine).

Abbreviations as in Table 1.

TABLE 3

ED Coefficients (mSv/mCi) Relating ED (mSv) to Administered Activity (mCi) for Myocardial Perfusion Imaging in Children and Adults

	Adult	15 Years	10 Years	5 Years	1 Year
Rb-82 chloride	0.041	0.052	0.11	0.18	0.31
N-13 ammonia	0.074	0.12	0.18	0.28	0.56
Tc-99m tetrofosmin (exercise	0.26	0.33	0.48	0.78	1.40
Tc-99m tetrofosmin (rest)	0.30	0.37	0.56	0.89	1.70
Tc-99m sestamibi (exercise)	0.29	0.37	0.59	0.85	1.70
Tc-99m sestamibi (rest)	0.33	0.44	0.67	1.00	2.00
F-18 fluorodeoxyglucose	0.70	0.89	1.40	2.10	3.50
Tl-201	5.2	7.4	21	29	35

Data from ICRP Publication 128 (48), with the exception of N-13 ammonia, for which data are from ICRP Publication 80 (46) in adults and ICRP Publication 53 (45) in children. To determine estimated effective dose (mSv), multiply administered activity (mCi) by appropriate coefficient in the table.

ED = Effective dose.

TABLE 4

Approaches for Dose Optimization of Cardiac CT Procedures in Children

Patient preparation
Heart rate–lowering medications should be considered for coronary imaging.
Pacemaker rate and mode should be adjusted for optimal imaging.
Sedation and/or anesthesia for suspended respiration in patients unable to cooperate may be needed when patient motion may affect image quality.
Contrast injection technique should be planned to simultaneously opacify all structures of interest in a single phase.
Scanner-based approaches
Scan range should be limited to the anatomy requiring evaluation.
Center the patient within the gantry.
Technique should be adjusted to:
Yield acceptable image quality that is tailored to the clinical indication.
Patient size: lower tube potential (kVp) settings can be used for most children.
Use of automated tube current and tube potential algorithms should be considered.
Scan mode chosen should provide diagnostic image quality at the lowest practical radiation dose.
Prospective ECG triggering should be used when possible.
ECG-gated tube current modulation should typically be used for functional imaging.
The narrowest temporal acquisition window possible should be used for coronary imaging.
Iterative reconstruction should be used on all scans.

CT = computed tomography; ECG = electrocardiogram.

TABLE 5

Approaches for Dose Optimization of Nuclear Cardiology Procedures in Children

• Stress-first/stress-only imaging for SPECT and PET myocardial perfusion imaging
• Multiple position imaging, to increase normalcy rate of stress-first imaging
• Rest imaging, when needed, performed on later day than stress imaging
• Avoidance of thallium-201
• Use of PET imaging tracers where available and appropriate
• Administered activity based on patient's age and/or habitus
• Use of advanced hardware (e.g., high-efficiency camera) or software (e.g., resolution recovery and noise reduction) technology to reduce administered activity
• Minimization of x-ray CT tube current for PET attenuation correction
• Use 3D acquisition mode for PET

3D = 3-dimensional; CT = computed tomography; PET = positron emission tomography; SPECT = single-photon emission computed tomography.

TABLE 6

Rules and Guidelines for Determining Administered Activity in Nuclear Cardiac Imaging Procedures in Children

	Formula for Activity in Child
North American Consensus Guidelines *	0.15 *mCi/kg for first Tc–99m dose in day* 0.45 *mCi/kg for second Tc–99m dose in day*
Clark's rule	$\text{Activity in adult} \cdot \frac{\text{Child's weight}}{150 \text{ lb.}}$
Young's rule	$\text{Activity in adult} \cdot \frac{\text{Age}}{\text{Age}+12}$
Webster's formula	$\text{Activity in adult} \cdot \frac{\text{Age}+1}{\text{Age}+7}$
Based on BSA	$\text{Activity in adult} \cdot \frac{\text{BSA}}{1.73\ m^2}$
EANM Dosage Card †	*Baseline Tc–99m Activity* (1.14 – 1.70 *mCi*)·*Weight–based Multiple*

Activity in adult for the first technetium-based radiopharmaceutical administered on a given calendar day is typically about 10 mCi. All ages are in years.

*North American Consensus Guidelines (87) provide recommendations only for Tc-99m sestamibi and tetrofosmin myocardial perfusion imaging, and not for other pediatric nuclear cardiology procedures. Minimum of 2 mCi for first dose of day, 6 mCi for second dose of day. Maximum of 10 mCi for first dose of day, 30 mCi for second dose of day.

†EANM Dosage Card provides recommendations only for Tc-99m sestamibi and tetrofosmin myocardial perfusion imaging, and not for other pediatric nuclear cardiology procedures. Weight-based multiples listed in EANM Dosage Card (88) include 2.71 for 10 kg, 4.86 for 20 kg, 6.86 for 30 kg, 8.86 for 40 kg, 10.71 for 50 kg, and 12.71 for 60 kg. Activity administered is recommended to be a minimum of 1.14 mCi and a maximum of 1.70 mCi, multiplied by the weight-based multiple, with a minimum recommended activity of 2.2 mCi regardless of weight. EANM Dosage Card specifies that minimum recommended activities are for standard cameras, but lower activities could be administered for high-efficiency cameras. Recommended activities determined using the EANM dosage card tend be higher than needed for diagnostic image quality in myocardial perfusion imaging and thus this approach is not recommended for determination of activity in children.

BSA = body surface area; EANM = European Association of Nuclear Medicine.

TABLE 7

Approaches for Dose Optimization of Fluoroscopically Guided Cardiac Procedures in Children: Hardware Features

Approach	Rationale
X-ray tube: Largest focal spot size: 0.8–1.0 mm; 80–90 kW	High kW rating ensures adequate radiation output for pediatric patients that are adult or near adult sized
Smallest focal spot size: ~0.3 mm; 12 kW	0.3-mm focal spot size is required to adequately support use of geometric magnification with minimal image blur
Maximum kW rating of the x-ray tube and generator match	Allows adequate penetration of adult or near adult-sized pediatric patients
Programmable age-appropriate radiological acquisition settings for patient sizes from 2–125 kg	Optimal settings vary depending on body habitus and region of body imaged
Multiple filters of varying thicknesses (spectral filtration) for insertion in x-ray beam (“beam hardening”)	Various filters, with atomic numbers greater than aluminum, inserted in the x-ray beam selectively remove low-energy, and pass high-energy x-rays to reduce skin dose
Virtual collimation to indicate graphically the location of the collimator blades or partial wedge filters without requiring fluoroscopy	Saves fluoroscopy time positioning collimators and wedge filters
Size of image receptors should be appropriate to the clinical practice	Although 23-cm image receptors are adequate for most adult cardiac catheterizations, larger format frontal plane image receptors (~35 cm) may be beneficial for pediatric imaging to visualize both lungs
Last image hold and last fluoro loop store/playback features	Allow images to be studied without further irradiation
Radiotranslucent patient comfort and positioning pads	Radio-opaque arm boards and other patient supports or pads can lead to artifacts in the image, increase scatter that reduces contrast in the image, reduce ability to penetrate large patients, and increase operator occupational dose from stray radiation

TABLE 8

Approaches for Dose Optimization of Fluoroscopically Guided Cardiac Procedures in Children: Software Configuration

Approach	Rationale
Select settings based on type of exam and patient size	Large patients may require maximum output of the fluoroscope. Small patients require different choices to manage dose and improve image quality
Select focal spot automatically based on patient size	Smallest focal spot size that provides adequate penetration improves visibility detail in the image
Keep pulse width ≤5 ms in small children and ≤10 ms in adolescent or adult patients	Short pulse widths freeze cardiac motion, which improves image sharpness of rapidly moving objects; longer pulse widths for adults improves penetration through thick body parts
Use algorithms for small children to reduce tube current or pulse width to prevent reduction of voltage below 60 kV	Voltages <70 kV do not improve contrast of iodine in the image but do unnecessarily increase patient dose rates relative to 70 kV
Select voltage and added filter thickness automatically as a function of patient mass	Filter thickness and voltage determine average energy of x-ray beam impinging on patient, which balances diagnostic image quality against well-managed patient doses depending on patient mass
Use AKIR α $1/(FOV)^{0.5}$ or constant based on pulse rate	KIR with flat panel detectors should follow AKIR α $1/(FOV)^{0.5}$ to manage patient dose while maintaining image quality. To manage AKIR with image intensifiers, the relationship is AKIR α 1/(FOV). For example, as the FOV is reduced by a factor of 2, this results in an increase of patient dose rate by a factor of 1.4 and 2.0 for the flat panel detector and image intensifier, respectively.

AKIR = air kerma rate at image receptor; FOV = field of view; KIR = kerma rate at image receptor.

TABLE 9

Approaches for Dose Optimization of Fluoroscopically Guided Cardiac Procedures in Children: Operator

Approach	Rationale
Select patient size and type of exam to manage acquisition parameters	Purpose of anatomic programming is to select configurable parameters to manage patient dose and image quality during exam.
Remove anti-scatter grid in children <20 kg	Patient dose rate is reduced with limited loss of image quality.
Remove extraneous body parts and other objects (e.g., arms, TEE probe) from the imaging FOV	Imaging through extraneous body parts and objects causes autoexposure controls to increase dose, and image quality is degraded.
Position patient at the imaging isocenter	Prevents anatomy of interest from shifting out of FOV as projection angles are changed and provides reasonable distance between x-ray tube and entrance plane of the patient.
Raise table to increase distance from radiation source (x-ray tube) to patient	Dose to the patient's skin decreases according to the inverse square law. In a biplane laboratory, table height may be limited by the need to position the patient for imaging with the lateral camera.
Minimize distance between patient and image receptor	A gap between exit plane of patient and image receptor requires more radiation at the patient and increases radiation dose. An exception is the air gap technique where receptor distance is increased and the anti-scatter grid is removed.
Start with a "low-dose" fluoroscopy mode selection and only increase (i.e., to moderate- or high-dose mode) if needed	Standards require at least 2 operator-selectable dose modes at table side (129). Operators can select a higher-dose mode if needed.
Pulsed fluoroscopy rates should not exceed 15 pulses/s	The lowest pulse rate that provides adequatetemporal resolution reduces dose to the patient. Slower pulse rates (10, 7.5, 3.5 pulses per second) may be adequate.
Acquisition (cineangiography) frame rates should not exceed 30 frames/s	Lower fame rates (e.g., 15 or 7.5 frames per second) should be considered for slower heart rates or when imaging slow-moving structures (e.g., venous angiography) to reduce patient dose.
Use collimation to reduce irradiated area. Include only necessary landmarks in image	Collimation improves image contrast and quality by limiting scatter radiation and reduces the irradiated area (volume) of the patient's body.
Use largest FOV (least electronic magnification)	Dose rates increase proportionately to the inverse of the FOV change (e.g., changing FOV from 20 cm to 12 cm increases dose rate 1.6 fold. Use of electronic magnification should be limited to critical times during a procedure when a magnified image is needed (e.g., manipulating a guidewire into a small vessel).
Avoid excessive use of oblique imaging angles	Oblique imaging requires the x-ray beam to pass through more tissue. This degrades image quality and causes autoexposure controls to increase radiation dose rate.
Limit beam "on" time: Use last image hold and last fluoro loop features when appropriate to avoid unnecessary fluoroscopy	Beam "on" time is directly proportional to dose.

FOV = field of view; TEE = transesophageal echocardiography.

TABLE 10

Approaches for Dose Optimization of Fluoroscopically Guided Cardiac Procedures in Children: Electrophysiology Procedures

Approach	Rationale
Use 3D EAM	Purpose of anatomic programming is to select configurable parameters to manage patient dose and image quality during exam.
Remove anti-scatter grid in children <20 kg	Patient dose rate is reduced with limited loss of image quality.
Remove extraneous body parts and other objects (e.g., arms, TEE probe) from the imaging field of view	Imaging through extraneous body parts and objects causes autoexposure controls to increase dose and image quality is degraded.
Position patient at the imaging isocenter	Prevents anatomy of interest from shifting out of field of view as projection angles are changed and provides reasonable distance between x-ray tube and entrance plane of the patient.
Raise table to increase distance from radiation source (x-ray tube) to patient	Dose to the patient's skin decreases according to the inverse square law. In a biplane laboratory, table height may be limited by the need to position the patient for imaging with the lateral camera.
Minimize distance between patient and image receptor	A gap between exit plane of patient and image receptor requires more radiation at the patient and increases radiation dose. An exception is the air gap technique where receptor distance is increased and the anti-scatter grid is removed.
Start with a "low-dose" fluoroscopy mode selection and only increase (i.e., to moderate- or high-dose mode) if needed	Standards require at least 2 operator-selectable dose modes at table side (129). Operators can select a higher-dose mode if needed.

3D EAM = 3-dimensional electroanatomic mapping; TEE = transesophageal echocardiography.